Bioorg. Med. Chem. 86 (2023) 117300

Contents lists available at ScienceDirect

Bioorganic & Medicinal Chemistry

journal homepage: www.elsevier.com/locate/bmc

Dual targeted 2-Benzylideneindanone pendant hydroxamic acid group exhibits selective HDAC6 inhibition along with tubulin stabilization effect

Kapil Kumar [a], Ranjana Das [a], Barsha Thapa [a], Bharti Rakhecha [b], Sapna Srivastava [b], Kumari Savita [a], Monazza Israr [a], Debabrata Chanda [a,c], Dibyendu Banerjee [b,c], Karuna Shanker [a,c], DU Bawankule [a,c], Benedetta Santini [f], Maria Luisa Di Paolo [d], Lisa Dalla Via [e], Daniele Passarella [f], Arvind Singh Negi [a,c,*]

[a] CSIR-Central Institute of Medicinal and Aromatic Plants, P.O. CIMAP, Lucknow 226015, India
[b] CSIR-Central Drug Research Institute, Sector-10, Jankipuram Extension, Sitapur Road, Lucknow 226031, India
[c] Academy of Science and Innovative Research (AcSIR), Ghaziabad, U.P. 201002, India
[d] Department of Molecular Medicine, University of Padova, via G. Colombo 3, 35131 Padova, Italy
[e] Department of Pharmaceutical and Pharmacological Sciences, University of Padova, via F. Marzolo 5, 35131 Padova, Italy
[f] Dipartimento di Chimica, Università degli Studi di Milano, Via Golgi 19, 20133 Milano, Italy

ARTICLE INFO

Keywords:
Acute oral toxicity
Anticancer
Antiinflammatory
Histone deacetylases
Leukemia
Microtubules

ABSTRACT

Abnormal epigenetics has been recognised as an early event in tumour progression and aberrant acetylation of lysine in particular has been understood in tumorigenesis. Therefore, it has become an attractive target for anticancer drug development. However, HDAC inhibitors have limited success due to toxicity and drug resistance concerns. Present study deals with design and synthesis of bivalent indanone based HDAC6 and antitubulin ligands as anticancer agents. Two of the analogues **9** and **21** exhibited potent antiproliferative activities (IC_{50}, 0.36–3.27 μM) and high potency against HDAC 6 enzyme. Compound **21** showed high selectivity against HDAC 6 while **9** exhibited low selectivity. Both the compounds also showed microtubule stabilization effects and moderate anti-inflammatory effect. Dual targeted anticancer agents with concomitant anti-inflammatory effects will be more attractive clinical candidates in future.

1. Introduction

Cancer is a complex multifactorial disease resulting from genetic and several environmental effects (epigenetic) involving multiple signalling pathways and factors like immune, angiogenesis, inflammation and kinase etc.[1] Over the years, it has become one of the most challenging diseases to human.[2] With the current arsenal of clinical drugs it could be managed to some extent but due to severe side effects, drug resistance and economic concerns, it has become a public health menace. Earlier, cancer drug development has been done based on single target ligands but now there is an era of multitargeted therapy, which is considered as more efficacious and less prone to drug resistance.[3,4] In initial approach two anticancer drugs with different mechanism of action were given in combination to tackle these problems, but many a times this approach was not sufficient due to enhanced drug burden and hence, exacerbated toxic effects to patients.[3,4] In the recent approaches, chimeric dual targeted ligands are being developed with double sword concept to tackle the problem.[5,6] It has given better results on efficacy front. However, toxicity remains a concern to these drugs which is relatively lower than the combination therapy approach.[3,4,7] In spite of some specific challenges, multitargeted drug development approach holds huge potential to achieve efficient and safer drug candidates particularly for cancer like complex diseases.[7] (see Fig. 1).

Cancer may be caused by genetic and/or epigenetic alterations leading to the dysregulation of several cellular pathways through diverse molecular mechanisms. In the recent years, epigenetics has been recognised as a key player in eukaryotic biological processes regulating gene expression. It is a reversible and inheritable process that acts on DNA and RNA methylation but without any change in their sequences post translational modifications (PTM) on histone, and expression of non-coding RNAs.[8] The *N*-terminal tail region of histones undergo several diverse enzyme modifications like acetylation, methylation,

* Corresponding author at: CSIR-Central Institute of Medicinal and Aromatic Plants, P.O. CIMAP, Lucknow 226015, India.
E-mail address: as.negi@cimap.res.in (A.S. Negi).

https://doi.org/10.1016/j.bmc.2023.117300
Received 9 March 2023; Received in revised form 19 April 2023; Accepted 23 April 2023
Available online 27 April 2023

phosphorylation etc. These PTMs have significant effects on gene expression and now also known as 'histone code'.[9] Histone acetylation and deacetylation plays an important role in the regulation of gene expression and in the modification of chromatin structure.[10] Thus, the expression of DNA is maintained by the acetylation and deacetylation.[11] This process is *via* an interplay between histone acetyl transferases (HATs) and histone deacetylases (HDACs) of histone protein.[12] So far eighteen different isoforms of nuclear and cytosolic HDACs have been identified in humans.[13] Based on the homology these have been classified in four different groups i.e. I (HDAC 1–3, 8, IIa (HDAC4,5,7,& 9), IIb (HDAC6 & 10), III (Sirtuins 1–7), and IV (HDAC11). Except class III, rest HDACs are Zn^{2+} dependent deacetylases.

As a consequence of epigenetic abnormality, over-expression of HDACs has been observed in various malignant tumours.[14–16] Epigenetic targeting has emerged as an efficacious therapy for haematological cancers. Over-expression of HDAC1 was found in lung,[17] gastric,[18] breast,[19] and prostate cancers,[20] HDAC2 and HDAC3 are over-expressed in colorectal cancer,[21] while cytosolic HDAC6 was up-regulated in breast cancer.[22] Owing to reversible nature of epigenetic dysregulation, these abnormalities can be rectified by some of the HDAC inhibitors. In the recent years, HDAC inhibitors have become a promising strategy to tackle cancer epigenetics.[23] In the last few years several HDAC inhibitors have been developed as clinical anticancer drugs specifically for hematologic cancers. Among these Vorinostat (SAHA) for cutaneous *T*-cell lymphoma,[24] Belinostat (PXD101, beleodaq) for peripheral *T*-cell lymphoma,[25] Romidepsin (FK228, Istodax) for *T*-cell lymphoma, Panobinostat (LBH-589, Farydak), for multiple myeloma[26] and Tucidinostat (CS-055, Chidamide) for the treatment of relapsed/refractory peripheral T cell lymphoma.[27] However, all these clinical drugs are non-selective HDAC inhibitors resulting in multiple side effects.[28]

In our previous studies, we designed and acquired a few microtubule destabilizers on indanone pharmacophore as anticancer agents.[29] Further, we wished to have some dual action antitubulin as well as HDAC6 inhibitors. Basically, histone deacetylase ligands are designed in five main chemical classes namely hydroxamic acids (Vorinostat, Belinostat and Panobinostat), benzamide (Tucidinostat), depsipeptide (Romidepsin), cyclic peptides and carboxylates. We adopted antitubulin indanone core as basic skeleton with a linker at C2 position and a hydroxamic moiety at the terminal of chain as zinc binding group to design the dual action pharmacophore. We prepared thirteen diverse compounds (**9, 10, 12, 21, 22, 26, 38–42, 46, 47**) on the indanone core and evaluated against three human cancer cell lines and one normal cell line (Vero). The most potent compound of the series was evaluated for detailed pharmacology, target studies (tubulin and HDAC), HDAC6 selectivity, cell cycle, antiinflammatory effect, confocal microscopy, and safety in rodent model.

2. Results

2.1. Chemical synthesis

The synthetic strategy was as depicted in Schemes 1-3. Indanone **4** was synthesized as per our previously reported method. Briefly, 3,4,5-trimethoxyacetophenone (**1**) was condensed with 3,4,5-trimethoxybenzaldehyde (**2**) in 3% alcoholic alkali to afford 1-(3,4,5-trimethoxyphenyl)-3-(3,4,5-trimethoxyphenyl) prop-2-en-1-one (**3**, chalcone). Chalcone **3** underwent Nazarov's cyclization in presence of trifluoroacetic acid at 110 °C to give 3-(3,4,5-trimethoxyphenyl)-4,5,6-trimethoxyindan-1-one (**4**).

Indanone **4** was condensed with 4-formyl-methylcinnamate (**5**) under alkaline medium to get a 2-benzylidene cinnamate derivative of indanone (**6**). Indanone ester **6** was hydrolysed in 3% aqueous-alcoholic (1:9) alkali to yield the corresponding carboxylic acid (**7**). The free carboxylic acid **7** was treated with tetrahydropyran (THP) protected hydroxylamine in presence of *N*-methylmorpholine/DMAP, *O*-THP-hydroxylamine and cyanuric chloride to get a corresponding protected hydroxamic acid derivative (**8**). The reductive deprotection of protected hydroxamic acid derivative **8** was done in presence of pTSA in dry methanol to get the final desired hydroxamic acid derivative (**9**). Derivative **9** was further acetylated to compound **10** in chloroform-DMAP-acetic anhydride system (Scheme 1).

For diversification at C2 substitutions, a few more C2-benzylidene derivatives were prepared on to indanone **4** to get the final hydroxamic acid derivatives (**21** and **22**) and also **26** as 2-benzylated derivative following the similar reaction conditions (Scheme 2).

For diversification at C2 substitutions, a few more C2-benzylidene derivatives without C3-aryl substitutions were also prepared on to indanones **27** and **28** to get the final hydroxamic acid derivatives (**38**–**40**). Further, 2-benzylated derivatives on catalytic hydrogenation yielded fully reduced hydroxamic acid derivatives (**44**, **45**, **48**, and **49**) (Scheme 3).

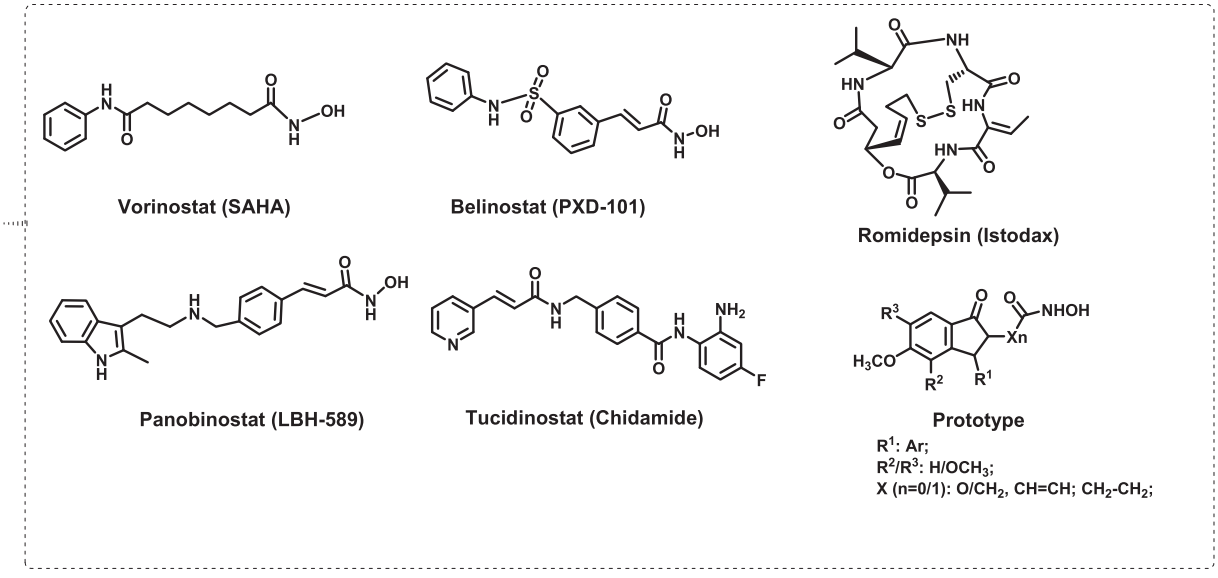

Fig. 1. HDAC inhibitors as clinical drugs and proposed prototype.

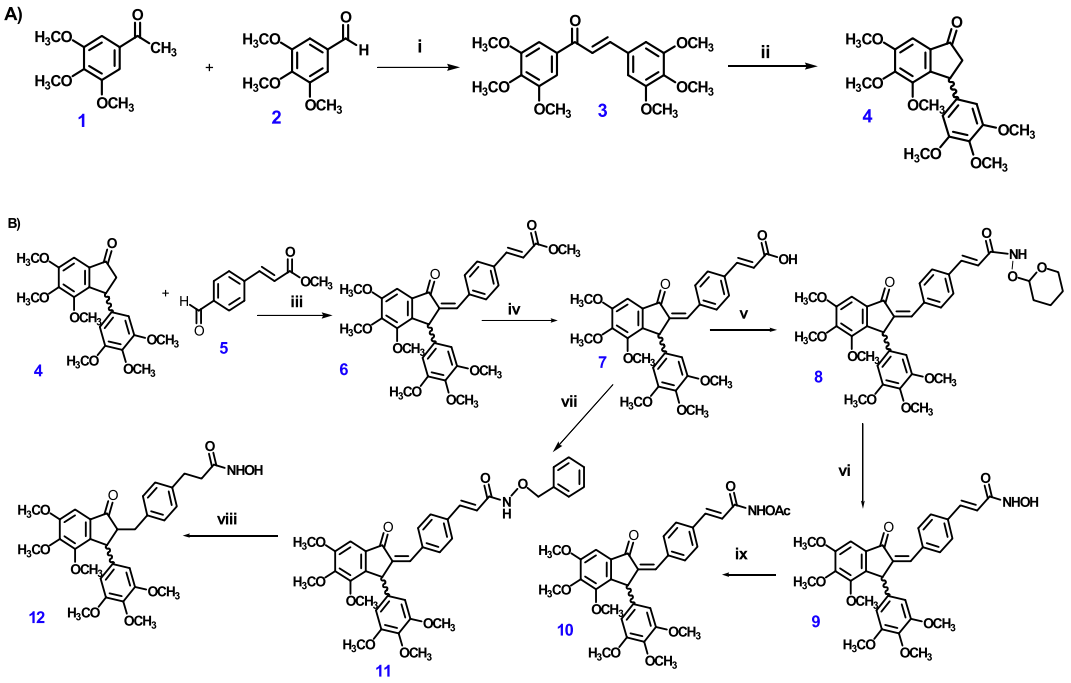

Scheme 1. Reagents and conditions: i) 3% KOH in MeOH, RT, 3 h, 92%; ii) TFA, sealed tube, 110 °C, 5 h, 35%; (iii) 3% KOH in MeOH, RT, 3–4 h, 79–92%; (iv) 3% KOH in MeOH-water (9:1), 50 °C, 2–3 h, 72–89%; v) Dichloromethane, *N*-methylmorpholine, TCT, *O*-THP, RT, 1–2 h,52–81%; vi) p-TSA, dry MeOH, RT, 30 min., 52–78%; vii) DMF, TEA, EDC-HCl, HOBt, NH_2OBn, 80 °C, 2–4 h, 60–81%; viii) DMF, 10% Pd-C/H_2, 2–3 h, 52–62%; ix) Dry $CHCl_3$, DMAP, Ac_2O, RT, 1 h, **23**: 58% & **10**: 92%.

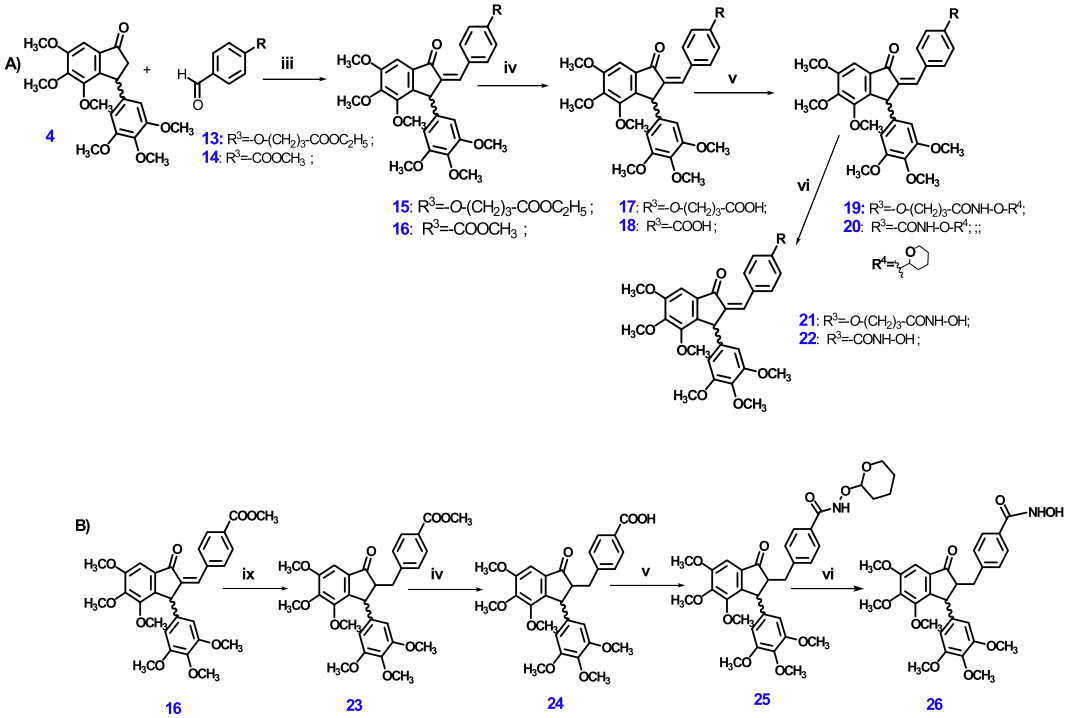

Scheme 2. Reagents and conditions: (iii) 3% KOH in MeOH, RT, 3–4 h, 79–92%; (iv) 3% KOH in MeOH-water (9:1), 50 °C, 2–3 h, 72–89%; v) Dichloromethane, *N*-methylmorpholine, TCT, *O*-THP, RT, 1–2 h,52–81%; vi) p-TSA, dry MeOH, RT, 30 min., 52–78%; ix) Dry $CHCl_3$, DMAP, Ac_2O, RT, 1 h, **23**: 58% & **10**: 92%.

2.2. Purity profile of compounds **9** and **21**

The purity of compound **9** was determined by RP-UPLC system using PDA detector range (190–400 nm) for co-elution of possible impurities. The purity of compound **9** was found to be 95.52% under the optimized chromatographic conditions. It was eluted at 7.745 min (t_R) as a sharp peak and peak integration was done at λ_{max} 340 nm. While, the purity profile of compound **21** was assessed by Shimadzu RP-HPLC using PDA detector with range (190–400 nm). It was detected at λ_{max} 360 nm and eluted as a sharp peak at 9.716 min (t_R). Under the optimized conditions the purity of compound **21** was found to be 93.27%.

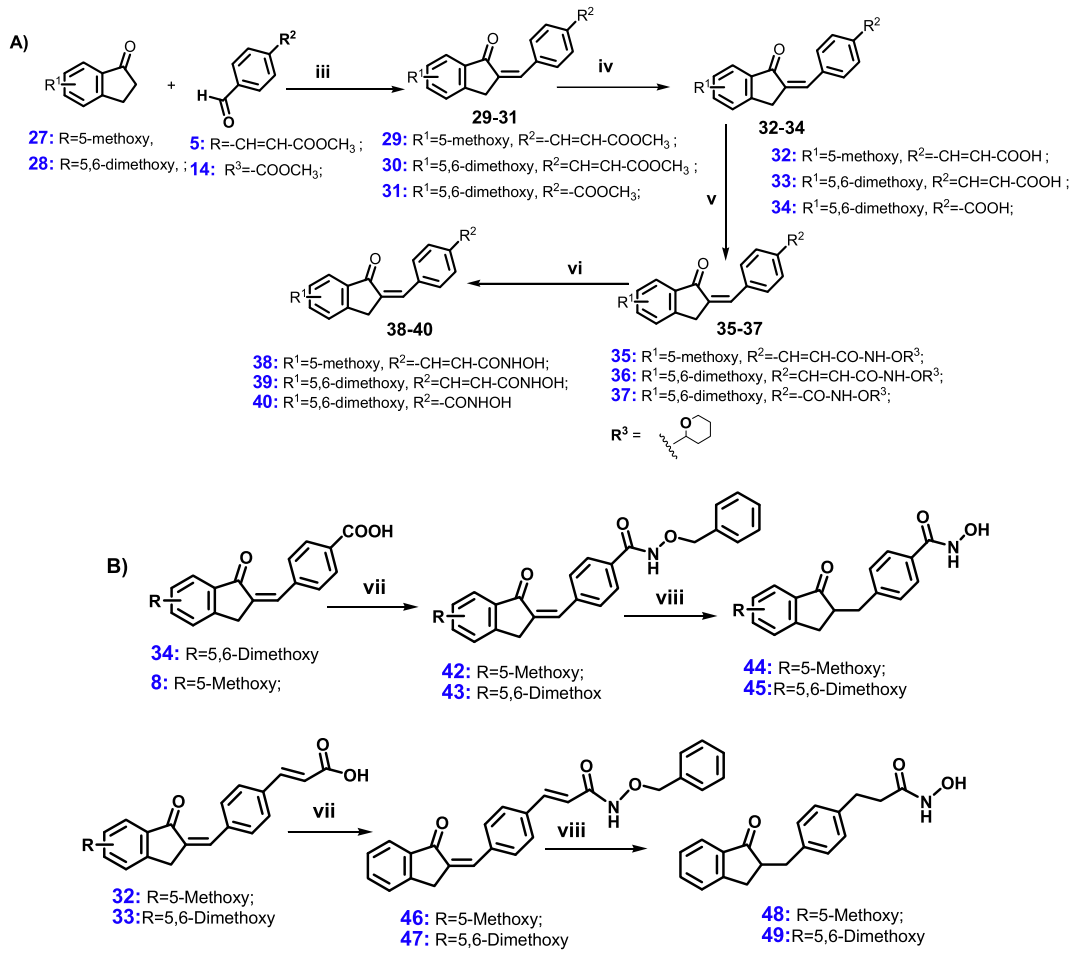

Scheme 3. Reagents and conditions: (iii) 3% KOH in MeOH, RT, 3–4 h, 79–92%; (iv) 3% KOH in MeOH-water (9:1), 50 °C, 2–3 h, 72–89%; v) Dichloromethane, *N*-methylmorpholine, TCT, *O*-THP, RT, 1–2 h,52–81%; vi) p-TSA, dry MeOH, RT, 30 min., 52–78%; vii) DMF, TEA, EDC-HCl, HOBt, NH_2OBn, 80 °C, 2–4 h, 60–81%; viii) DMF, 10% Pd-C/H_2, 2–3 h, 52–62%.

2.3. Biological evaluation

2.3.1. Antiproliferative activity

All the indanone based hydroxamic acid derivatives (**9**, **10**, **12**, **21**, **22**, **26**, **38**–**40**, **42**, **43**, **46**, **47**) were evaluated for *in-vitro* cytotoxicity by Sulphorhodamine assay against human cancer cell lines MCF-7 (Hormone dependent breast), MDA-MB-231 (Triple negative breast cancer), K-562 (Chronic myelonoid leukemia) and a normal cell line Vero (African green monkey kidney cells) (Table 1). Doxorubicin, Podophyllotoxin, Tamoxifen and Tubastatin A were used as positive controls.

2.3.1.1. Structure activity relationship. There were two types of indanone series; Series I was 4,5,6-trimethoxy-3-(3,4,5-trimethoxyphenyl) 1-indanone; while Series II was 5-methoxy/5,6-dimethoxyindanone. In general Series I compounds possessed high to moderate antiproliferative activity against both MDA-MB-231 and K562 cell lines. While, Series II compounds showed moderate to low efficacy. In both the Series, reduction of unsaturated double bonds was not favourable to bioactivity as it yielded compounds with relatively lower activity (Compounds **9** Vs **12**;compounds **22** Vs **26**) and In series II, (Compounds **11**, **12**, **23**–**26** and **38**–**40;** compounds **40** Vs **45**).

In series I, carbon chain C3 or more at C2-benzylidene ring was favourable for cytotoxicity (MDA-MB-231: Compounds **9**, IC_{50} = 0.36 μM; **21**, IC_{50} = 3.25 μM; K562: Compounds **9**, IC_{50} = 3.27 μM; **21**, IC_{50} = 1.66 μM). It was also observed that compounds with oxygenated carbon chain at C2-benzylidene ring were more cytotoxic against K562 cell line as compared to MDA-MB-231 cell line. As compounds **21** was more effective against K562 cell line as compared to MDA-MB-231 cell line.

A 3,4,5-trimethoxyphenyl ring at C3 position seems a preferred substitution for better efficacy. A restricted rotation at C2 as benzylidene is a better arrangement. Also, all the hydroxamic acid benzyl esters exhibited insignificant cytotoxicity.

2.3.2. Cell cycle analysis

Uncontrolled proliferation of cells is one of the remarkable hallmarks of cancer. Oncogenic process exerts its prominent effect on targeting genes those regulate cell cycle.[30] The effect of compound **21** was observed on triple negative breast cancer (MDA-MB-231) cell line at three different concentrations i.e. 1.625 μM (Half IC_{50}), 3.25 μM (IC_{50}), and 6.5 μM (2*IC_{50}). The standard drug doxorubicin was taken at 0.285 μM (1/2*IC_{50}), 0.57 μM (IC_{50}), and 1.14 μM (2*IC_{50}). In cell cycle analysis compound **21** exhibited mainly S phase arrest. It also showed slight G2/M phase arrest. Doxorubicin also exhibited S phase arrest.

In K562 leukemic cells, the effect of both the compounds **9** and **21** was not very prominent. However, in case of compound **9**, there was slight effect on G1/S phase arrest while compound **21** showed S phase arrest. The cell cycle analysis clearly indicates that the compound **21** induces apoptosis *via* multiple mechanisms. Perhaps, it is a dual targeted anticancer agent. Both the compounds clearly showed induction of apoptosis (Fig. 2).

2.3.3. Histone deacetylase 6 inhibition activity

The capability of the compounds to inhibit the histone deacetylase enzyme activity was evaluated in HeLa nuclear extract, containing both

Table 1
Antiproliferative activity of indanone based hydroxamic acid derivatives against human cancer cell lines and normal cell line.

Sample code	Cytotoxicity (IC_{50} in μM)				Selectivity index (SI) IC_{50}(Vero)/ IC_{50}(K562)
	MCF-7	MDA-MB-231	K562	Vero	
9	>100	**0.36 ± 0.04**	**3.27 ± 0.63**	100.32 ± 6.89	30.68
10	75.05 ± 2.86	**19.05 ± 1.91**	23.64 ± 1.04	47.49 ± 1.20	2.01
12	52.32 ± 1.74	**20.67 ± 3.45**	51.87 ± 2.35	76.20 ± 10.17	1.47
21	49.67 ± 2.79	**3.25 ± 0.84**	**1.66 ± 0.53**	47.23 ± 1.20	28.45
22	60.1 ± 1.26	>100	47.69 ± 2.73	72.25 ± 6.30	1.51
26	87.52 ± 4.07	>100	36.78 ± 2.99	91.82 ± 6.68	2.50
38	97.52 ± 4.14	>100	>100	100.37 ± 12.99	≤1.0
39	>100	>100	>100	128.52 ± 6.62	>1.0
40	>100	>100	46.92 ± 0.44	88.37 ± 16.75	1.88
44	55.25 ± 1.13	28.80 ± 1.52	**18.58 ± 1.59**	55.52 ± 2.99	2.99
45	>100	>100	>100	193.08 ± 37.80	>1.93
48	93.85 ± 1.51	>100	61.78 ± 0.51	114.19 ± 10.91	1.85
49	51.67 ± 0.45	32.61 ± 1.41	30.39 ± 3.93	48.66 ± 1.69	1.60
Doxorubicin	2.58 ± 0.12	0.57 ± 0.11	5.23 ± 1.76	1.87 ± 0.63	0.36
Podophyllotoxin	10.04 ± 0.74	20.22 ± 1.37	18.39 ± 3.25	ND	ND
Tamoxifen	10.74 ± 0.27	18.48 ± 1.53	ND	36.20 ± 12.42	ND
Tubastatin A	ND	ND	2.07 ± 0.53	ND	ND

*n = 3; incubation time: 72 h; ND, not determined.

classes I and II enzymes (PanHDAC), and on human recombinant HDAC6 (class II enzyme) and the obtained results are reported in Table 2. Preliminarily, all compounds were tested at 20 μM concentration on nuclear extract and the residual enzyme activity, determined with respect to the control sample (without treatment), was evaluated. Trichostatin A, a non-selective HDAC inhibitor, and Tubastatin A, a highly selective HDAC6 inhibitor, were used as reference (Positive controls). Standard anticancer drug doxorubicin was used as negative control (no HDAC inhibition).

Among the evaluated analogues, compounds **9**, **21**, **26** and **47** showed high inhibitory potency, when tested on HeLa nuclear extracts, containing both class I and II HDAC activity (PanHDAC), with residual enzyme activity lower than 0.40, i.e. 60% of enzyme inhibition. Interestingly, for compound **21** an effect similar to that of Trichostatin A was found, while for compound **9** was obtained about 90% HDACs inhibition that is an inhibitory potency even higher than that observed for the reference inhibitor.

The above derivatives at 20 μM concentration maintain or increase the inhibitory potency also on the recombinant HDAC6 enzyme, like, in addition, compounds **38**, **42** and **43**. In fact, for all these compounds a percentage of inhibition of enzyme activity higher than 90% was observed. The calculation of HDAC6 selectivity, i.e. the ratio between the residual activities PanHDAC/HDAC6 at 20 μM concentration of test compound, highlighted for **21**, **26**, **38** and **42** a high selectivity toward HDAC6, that is HDAC6 residual activity more than seven folds lower than the residual activity obtained on HeLa nuclear extracts (Table 2).

The most interesting compounds (**21**, **26**, **38**, and **42**), endowed with high inhibitory potency and selectivity towards HDAC6, were further tested on the recombinant enzyme at 2 μM concentration. The obtained results (Table 2) confirmed the remarkable inhibitory potency event though lower than that exerted by the reference Tubastatin A.

Finally, a comparison of the results showed in Table 2, highlights compounds **9** and **21** as the best inhibitors on PanHDAC (classes I and II) and compound **21** more selective than compound **9** for HDAC6. In addition, compounds **26** and **42** showed the highest effect and selectivity on HDAC6, even if their inhibitory potency on PanHDAC from nuclear extracts is significantly lower than that induced by **9** and **21**.

2.3.4. *Tubulin kinetics of compounds **9** and **21***

Tubulin has been considered one of the most prominent targets for anticancer drug development. Both microtubule stabilizer and microtubule destabilizers disrupt tubulin-microtubule dynamic equilibrium and eventually induce cell cycle arrest.[31] In the tubulin kinetics study, compound **21** showed stabilization effect on tubulin polymerisation. However, its stabilization effect was slightly less than paclitaxel (Standard stabilizer). Podophyllotoxin exhibited strong destabilization effect.

Fig. 3, the first part shows curves of paclitaxel (5 μM) and compound **9** (0.2, 1.0 & 5 μM). Fig. 3 shows paclitaxel curve above the GTB (General tubulin buffer) containing GTP protein clearly showing stabilization effect. The curve of podophyllotoxin below the GTB protein curve, exhibits strong destabilization effect on tubulin polymerisation process. Compound **9** showed stabilization effects. In second part of Fig. 3 the effect of compound **21** at 0.2 μM concentration was negligible i.e. not clear. However, at 1 μM and 5 μM concentrations it showed clear stabilization effect on tubulin polymerisation. The stabilization effect of both the compounds **9** and **21** was better than paclitaxel at 5 μM.

2.3.5. *Effect of compounds **9** and **21** on actin-cytoskeleton structure by confocal microscopy*

In tubulin kinetics experiment, compounds **9** and **21** exhibited microtubule stabilization effect. In order to confirm the phenotypic effect also on cellular cytoskeletal network of actin and tubulin, HeLa cells were incubated for 4 h with both compounds, immunostained and analysed under confocal microscope. Paclitaxel and podophyllotoxin were taken as stabilizer and destabilizer references respectively. The most representative microphotographs are showed in Fig.. 4. The results indicate that **9** and **21** at 5 μM and 10 μM induce an effect on cellular cytoskeletal network of tubulin similar to that of paclitaxel, confirming the microtubule stabilization effect.

2.3.6. *Molecular docking studies*

(a) *Interaction of **9** and **21** with β-tubulin*

The *in-silico* molecular interaction studies were done of both the potential candidates with β-tubulin protein (Table 3, Fig. 5). Surprisingly, both the ligands occupied laulimalide binding pocket of β-tubulin. Both the synthesized ligands i.e. **9** and **21** showed good affinity towards the target protein. The docking studies suggested that both synthesized compounds had good interaction with β-tubulin. The observed docking scores were −9.1 Kcal/mol, and −7.7 Kcal/mol for **9** and **21** respectively while for positive control laulimalide showed −8.8 Kcal/mol binding energy. There were eleven residual amino acids common to all the three ligands which clearly indicated that these occupied the same binding pocket. However, laulimalide and **9** showed better binding affinity due to two additional H-bonds.

(b) *Interaction of **9** and **21** with HDAC 1 & 6 enzymes*

For docking studies, Trichostatin A, a non-selective inhibitor of HDAC was selected as positive control for HDAC interaction study and Tubastatin A, a highly selective inhibitor of HDAC6 as positive control for HDAC6 interaction study (Table 4, Fig. 6). Docking results showed that in case of HDAC1 enzyme, all the three ligands did not occupy the

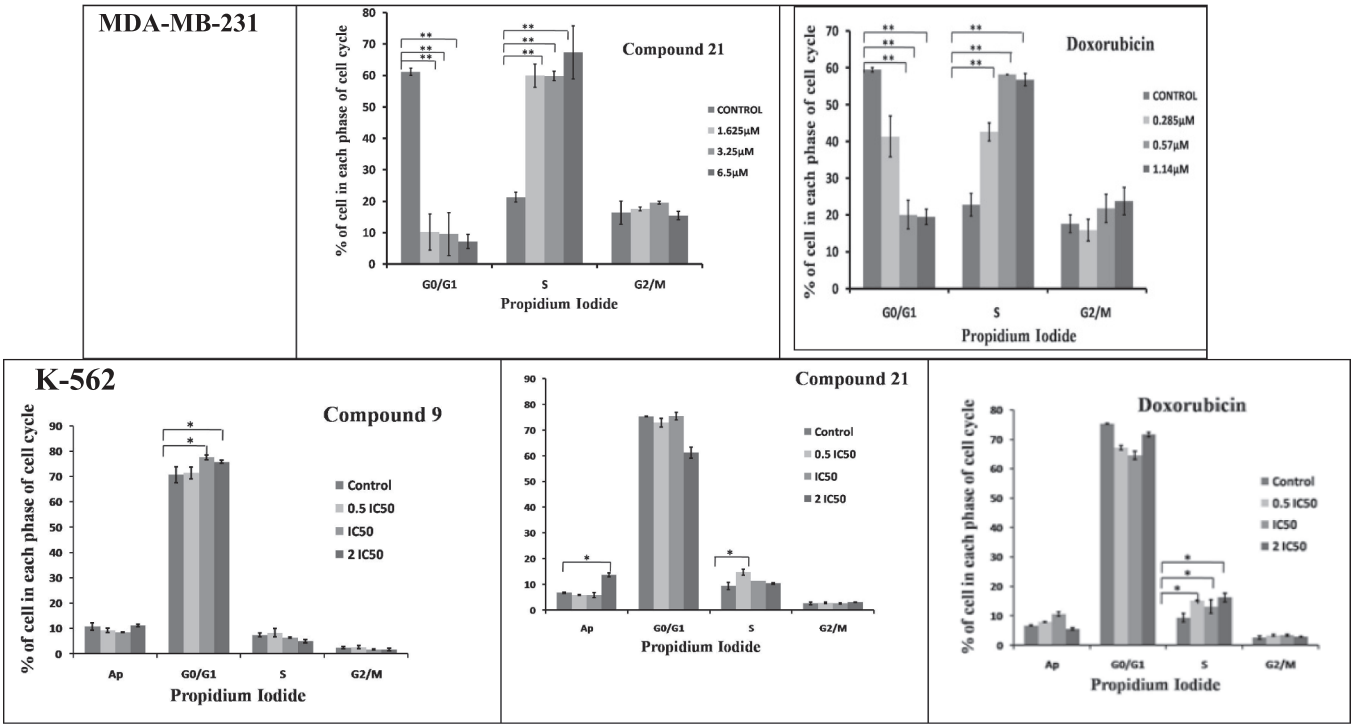

Fig. 2. A) MDA-MB-231 (TNBC cells) were grown in the presence of HDAc inhibitor compound **9, 21** anddoxorubicin for 24 h. It was found that both the compounds **9** & **21** induced mainly S-phase arrest the cells at all the tested concentrations of 1.625 μM, 3.25 μM, and 6.5 μM. Both are potent inhibitors of DNA replication which occurs in the S-phase of cell cycle. Doxorubicin was used as positive control. It also induced S-phase arrest. b) K562 cells were grown in the presence of HDAC inhibitor compound **21** for 24 h. It was found that the compound was able to arrest the cells in S-phase at all the tested concentrations of 1.625 μM, 3.25 μM, and 6.5 μM of **21**. The compound is therefore a potent inhibitor of DNA replication which occurs in the S-phase of cell cycle. Doxorubicin was used as positive control.

same binding pocket. Trichostatin A and **9** occupied similar binding pocket but **21** has nearby different binding pocket.

Interestingly, in case of HDAC6 binding, Tubastatin A and compound **21** occupied same binding pocket as out of fifteen residual amino acids, twelve (HIS463, SER531, TYR745, ASP705, GLY743, HIS614, HIS573, HIS574, LEU712, PHE643, GLY582, PHE583) were common to both, while **9** occupied different binding pocket. However, the binding affinity of compound **21** was less than the standard compound Tubastatin A indicating relatively inferior efficacy. Overall, it can be concluded that **21** is a selective inhibitors of HDAC6 while **9** is a non-selective inhibitors of HDAC6.

(c) *In-silico prediction of physicochemical properties of compd **21***

Physicochemical properties of a compound impart an assessment about the druggability of the candidate. These are the intrinsic physical and chemical characteristics of a compound. The drug candidate has to pass through various barriers and biological mediums for eliciting a biological response. It must reach in sufficient concentration at target site to elicit the desired pharmacological response in the body.

We predicted the important physicochemical properties of the selective HDAC6 ligand i.e. compound **21** using SwissADME software (Table 5). Tubastatin A was used for comparison. Compound **21** displayed some of the properties in satisfactory limits, but it deviated 'Lipinski rule' for two parameters (Molecular weight & H-bond acceptors), polar surface area (TPSA) was also beyond higher limits, rotable bonds and molar refractivity. Overall bioavailability was speculated quite low. However, it did not show any PAINS alert which otherwise indicates possibility of false positive results in *in-vitro* assays. Bioavailability radar shows slight deviation due to higher number of rotable bonds (more flexibility) in the chemical structure of the compound (Fig. 7).

[Six physicochemical properties are taken into account: lipophilicity, size, polarity, solubility, flexibility and saturation. The pink area represents the optimal range for each properties (lipophilicity, MW, polarity, TPSA solubility as log S, saturation: fraction of carbons in the sp^3 hybridization, and flexibility as rotatable bonds. In this example, the compound **21** is predicted to be poorly bioavailable, needs to be improved for this].

2.3.7. *Antiinflammatory effect of compounds **9** and **21***

Tumour microenvironment is an important feature while eradicating tumour. It has a decisive role in tumour differentiation, tumour epigenetics, and immune evasion. The success of chemotherapy relies to a great extent on the knowledge of tumour microenvironment. Tumour inflammatory cells (cytokines, chemokines & prostaglandins) are an integral part of tumour microenvironment and these are over-expressed during the pathogenesis of the disease.[32] Both TNF-α and IL-6 are well established prognostic markers in acute cancer inflammation.[33] Compound **9** exhibited moderate anti-inflammatory effect on LPS induced proinflammatory cytokines, by lowering TNF-α (17–29%) and IL-6 (13–27%) However, compound **21** exhibited low antiinflammatory effect, TNF-α (12–15% only) and IL-6 (9–12% only) at 1 μg/mL and 10 μg/mL concentrations (Table 6). While, dexamethasone, the standard drug showed 52% and 40% inhibition at 1 μg/mL against both the parameters respectively.

2.3.8. *Safety studies*

Owing to its potent anticancer efficacy, compound **9** was further evaluated for its safety aspects *via* acute oral toxicity in rodent model (Table 7, Fig. 8). For this study four different oral doses i.e. 5 mg/kg, 50 mg/kg, 300 mg/kg and 1000 mg/kg were ingested to Swiss albino mice. No morbidity, mortality or any behaviourable changes recorded during the experimental period of seven days. Hematological and serum biochemical parameters studied at the end of the experiment showed non significant changes in all the parameters studied. Gross pathological

Table 2
Pan HDAC and HDAC6 enzyme activity of indanone based hydroxamic acid derivatives.

Sample code	Residual HDACs activity PanHDAC (20 μM)	Residual HDAC6 activity (20 μM)	Residual HDAC6 activity (2 μM)	[b]Inhibitory potency on PanHDAC [c]Selectivity for HDAC6
Control	1.00 ± 0.09	1.00	1.00	–
9	**0.09 ± 0.01**	**0.09 ± 0.01**	–	High potency Low selectivity
10	1.04 ± 0.14	0.19 ± 0.02	–	Not active
12	0.51 ± 0.07	**0.18 ± 0.02**	–	Moderatepotency Moderate selectivity
21	**0.23 ± 0.05**	**0.03 ± 0.02**	**0.68 ± 0.12**	**High potency High selectivity**
22	1.03 ± 0.15	0.95 ± 0.05	–	Not active
26	**0.37 ± 0.05**	[a]**nd**	0.30 ± **0.04**	**High potency, High selectivity**
38	0.77 ± 0.10	0.09 ± 0.01	0.96 ± 0.9	Low potency High selectivity
39	1.11 ± 0.15	0.62 ± 0.04	–	Not active
40	0.78 ± 0.12	**0.11 ± 0.01**	–	Low potency High selectivity
42	0.63 ± 0.17	**nd**	0.32 ± 0.05	Low potency High selectivity
43	0.82 ± 0.13	0.08 ± 0.01	–	Low potency High selectivity
46	0.49 ± 0.11	0.14 ± 0.02	–	Moderate potency Moderate selectivity
47	**0.32 ± 0.05**	**0.08 ± 0.01**	–	**High potency Moderateselectivity**
Doxorubicin	1.29 ± 0.14	–	–	Not active
Trichostatin A	0.17 ± 0.03	–	**0.09 ± 0.02**	High potency Low selectivity
Tubastatin A	0.35 ± 0.09	**nd**	**>0.01**	High potency High selectivity

[a] nd = none detectable residual activity (<0.01).
[b] Inhibitory potency on PanHDACsat 20 μM concentration of test compound:<0.40 = high potency; 0.41–0.60 = moderate potency; >0.60 = low potency.
[c] Selectivity for HDAC6 is defined by the ratio between the residual activities PanHDAC/HDAC6 at 20 μM concentration of test compound:PanHDAC/HDAC6 ≥ 7 = high selectivity, PanHDAC/HDAC6 6.9–2.5 = moderate selectivity, PanHDAC/HDAC6 < 2.5 = low selectivity; Trichostatin A non selective, Tubastatin A highly selectine HDAC6 inhibitors.

observation recorded non observable changes in the major organs studied including their absolute and relative organ weight. Overall the tested compound **9** has a 'no observed adverse effect level (NOAEL)'. However, sub-acute and chronic experiments are also suggested to see the effect of drug candidate on repeated exposure.

3. Discussion

Anticancer drugs resistance is a complex process that arises from altering in the drug targets. Multitargeted approach is considered a better approach to overcome with drug resistance with enhanced efficacy.

In our studies, we designed the molecules based on two different biological targets; i) beta tubulin protein and ii) Histone deacetylase 6 enzyme. Both the lead compounds **9** and **21** exhibited significant microtubule stabilization effect. Both tubulin kinetics assay and confocal microscopy confirmed this effect. Microtubules are essential components of eukaryotic cytoskeleton having crucial role in cell shaping, intracellular transport, motility and chiefly the cell division in mitotic phase. Tubulin-microtubule dynamics equilibrium is an important phenomenon nevertheless, any disturbance leads to cell cycle arrest. Further, post-translation modifications (PTMs) also control functions of MT cytoskeleton also known as 'Tubulin code' which is in fine tune and has been linked to several types of cancer due to dysfunction.[34]

Acetylation and deacetylation of alpha tubulin (Lysine 40) is also linked with PTMs of tubulin which is an epigenetic factor in cancer progression. Both the compounds **9** and **21** possessed potent HDAC inhibition activity. However, **30** showed high selectivity to HDAC6. There are about eighteen isotypes of HDAC enzyme and high selectivity is required to reduce the toxicity of the drug candidates.[13] Thus, the high selectivity of **30** designates it a better candidate as compared to **9**. There are HDAC inhibitors like Trichostatin A exhibiting high potency but low selectivity against HDAC6[35] while Tubastatin A depicting both high potency and high selectivity against HDAC6.[36]

In cell cycle analysis, compound **21** prominently induced S phase arrest and poorly G2/M phase arrest in MDA-MB-231 cells. However, induction of apoptosis in leukemic cell line was very poor. S-phase arrest indicates that **21** interferes in the duplication of DNA. Generally, chemotherapeutics target proliferating cells *via* interference in the DNA replication in S phase.[37] Another class of drugs known as antimitotic drugs interfere in tubulin microtubule dynamics and stops cell replication in mitosis.

In tubulin kinetic, **21** showed potential stabilization effect on microtubule dynamics. Its stabilization effect was quite comparable to

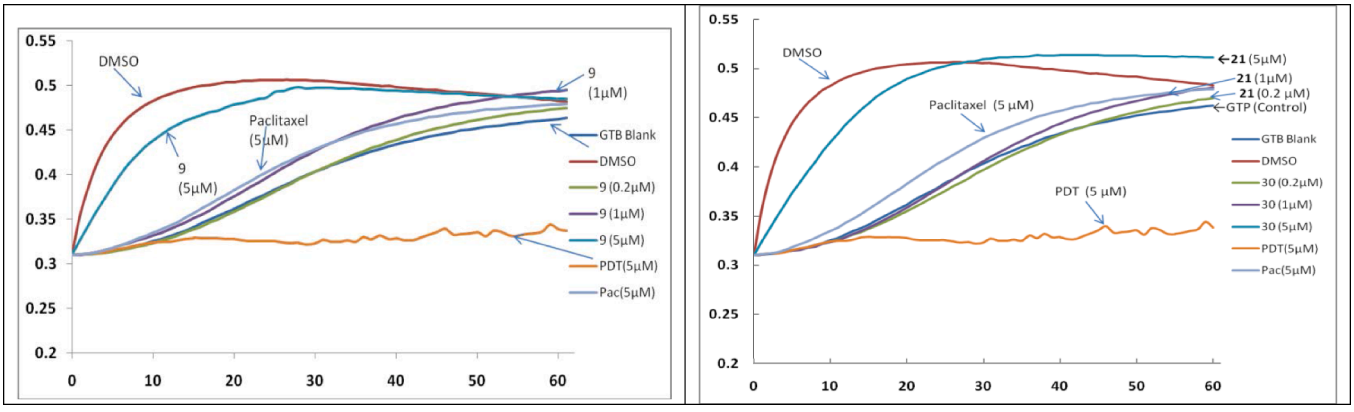

Fig. 3. A) Tubulin kinetic graph of compound **9** at 0.2 μM, 1 μM, and 5 μM concentrations, while Podophyllotoxin (PDT, standard destabilizer) & Paclitaxel (Pac, standard stabilizer) at 5 μM. Line below GTP indicates destabilization while lines above GTP show stabilization effects. Compound **9** clearly indicates significant stabilization effect. b) Tubulin kinetic graph of Compound **21** at 0.2 μM, 1 μM, and 5 μM concentrations, while Podophyllotoxin (PDT, standard destabilizer) & Paclitaxel (Pac, standard stabilizer) at 5 μM. Line below GTP indicates destabilization while lines above GTP show stabilization effects. Compound **21** clearly indicates significant stabilization effect.

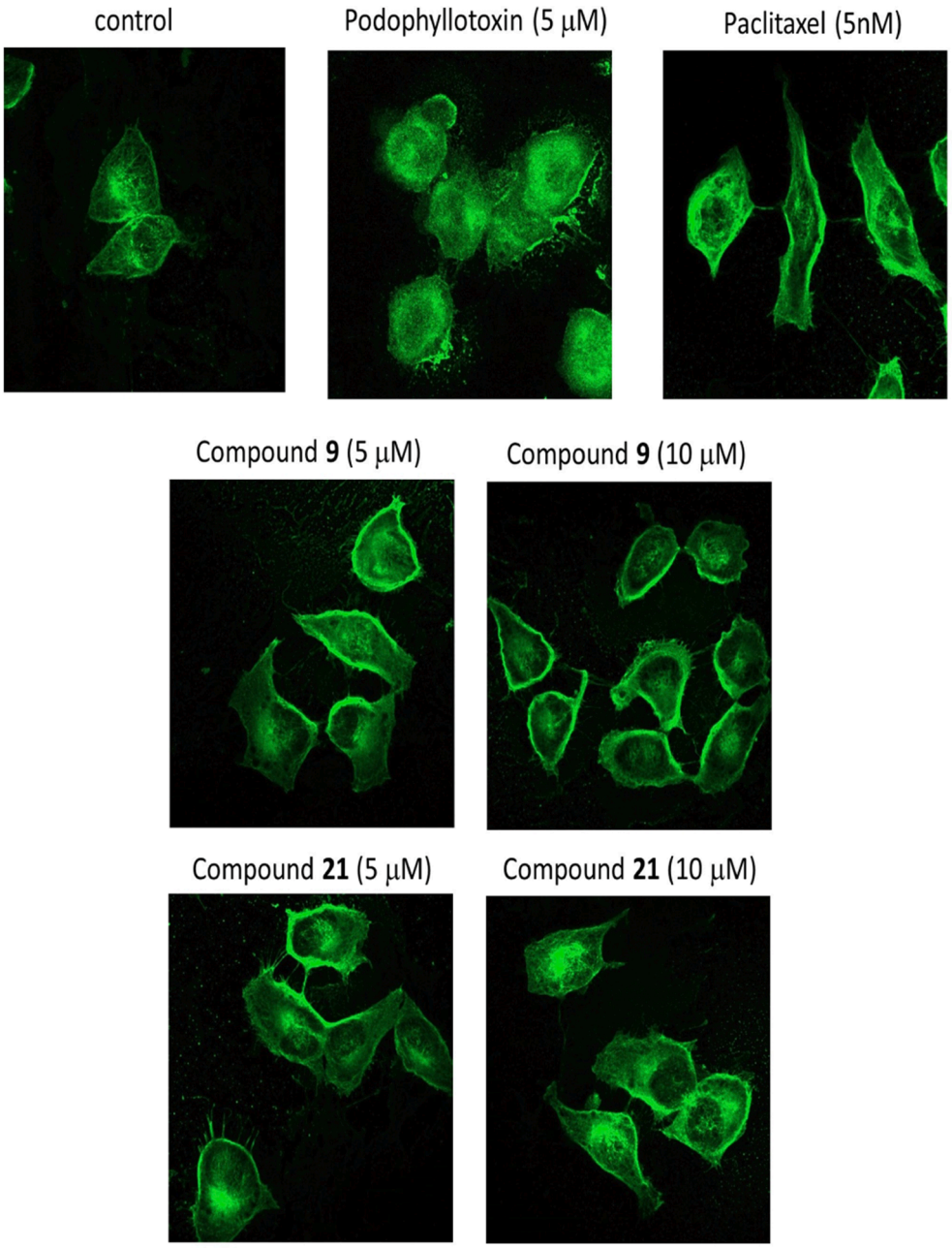

Fig. 4. Effect of **9** and **21** on microtubules of HeLa cells treated for 4 h with compounds at 5 and 10 μM concentrations. Microtubules were stained with anti-β-tubulin antibody conjugated to Alexa Fluor® 488. Paclitaxel (5 nM) and podophyllotoxin (5 μM) were taken as references.

stabilization effect of paclitaxel at same concentration. This stabilization effect was further confirmed by confocal microscopy which gives a phenotypic effect of compounds on microtubules in HeLa cells. Extremely dynamic mitotic spindle microtubules are remarkable therapeutic targets for chemically diversified and clinically successful anticancer drugs.[31,38,39] Generally, microtubule stabilizers bind with microtubule and disturb its dynamic equilibrium during mitosis which eventually induces apoptosis.[40,41]

Molecular docking studies exhibited interaction of both the candidates with β-tubulin. Both the ligands occupied laulimalide binding pocket with good affinity. There were eleven common amino acid residues indicating that these occupied the same binding pocket. Further, both the ligands also showed affinity of histone deacetylases 1 & 6. On comparison it was concluded that **9** occupies mainly HDAC1 quite similar to Trichostatin A which is a non-selective HDAC inhibitor while, **21** binds to HDAC6 quite similar to Tubastatin A which is a selective inhibitor of HDAC6. On biochemical evaluation, **9** was non selective inhibitor of HDAC6 while **21** was found to be selective inhibitor of HDAC6.

Thus, **21** exhibited dual targeted potent antimitotic and selective HDAC6 inhibition effects. However, **9** exhibited antimitotic and non-selective HDAC6 activity. Uncontrolled cell proliferation is the hallmark of cancer, and tumor cells have typically acquired damage to genes that directly regulate their cell cycles. Several proteins control the timing of the events in the cell cycle, which is tightly regulated to ensure that cells divide only when necessary. The loss of this regulation is the hallmark of cancer.

'Safety pharmacology' is an important aspect that regulatory authorities require for an investigational drug. The drug safety issues have become quite prominent in drug research.[42] Acute oral toxicity is a short term evaluation of adverse effect of a drug candidate on administration *via* oral route.[43] Compound **9** did not show any significant toxicity

Table 3
Binding energy, hydrogen bonding, and active binding site residues observed in the *in silico* docking studies of ligands **9** and **21** with selected target (PDB ID:4O4H).

Protein & Ligands	Binding Affinity (Kcal/mol)	H-Bonding	Amino acid residues (4Å)
Laulimalide	-8.8	ARG369, THR276	VAL23, ARG320, ALA233, GLU27, SER236, GLY237, THR376, SER374, PHE272, PRO274, ARG369, PRO360, THR276, LEU371, GLY370, HIS229
9	-9.1	SER374, THR376	GLN282, ARG369, THR276, SER277, GLY370, ARG320, PHE272, SER374, ALA375, SER236, THR376, PRO360,VAL23, LEU371, GLY237, ALA233, HIS229, SER232, LYS19, GLU22
21	-7.7	----	ALA375, ALA273, LEU371, SER232, LYS19, HIS229, SER277, GLY225, ASP226, PRO82, GLU22, ARG369, VAL23, ALA233, THR234, PRO360,GLY237, SER236, ARG320, THR376, PHE272, SER374

[Residual amino acids- with blue font, common to all three; with pink font, common to Laulimalide and **9** with green font, common to Laulimalide and **21**; There are eleven common residual amino acids clearly indicating the same binding pocket occupied by all the three ligands].

during acute oral toxicity. Over all the tested compound **9** has a 'no observed adverse effect level (NOAEL)'. It was well tolerable and quite safe. However, sub-acute and chronic experiments are also suggested to see the effect of drug candidate on repeated exposure. Being an essential part of modern drug development, WHO has termed it as 'Pharmacovigilence' and defined as the science and activities related to the detection, assessment, understanding and prevention of adverse drug effect or any other possible drug related problems.[44]

4. Conclusion

In the present study, a dual targeted pharmacophore was designed and some representative compounds were synthesized as effective anticancer agents. The potential candidates **9** and **21** exhibited microtubule stabilization and HDAC6 inhibitory effect. However, the HDAC 6 inhibition by **21** was highly selective but **9** was non-selective. **21** also possessed low antiinflammatory effect. The candidate molecule was well tolerable and safe in rodent models. Further optimization of the core is underway which may yield some better candidate drugs in future.

5. Experimental methods

5.1. Chemical synthesis

5.1.1. Synthesis of 2,3-Dihydro-4,5,6-trimethoxy-3-(3,4,5-trimethoxyphenyl)inden-1-one (4)

The synthesis of hexamethoxyindanone (4) was done as per our previously reported method.[45] Briefly, gallic acid was modified to 3,4,5-trimethoxybenzaldehyde and 3,4,5-trimethoxyacetophenone and condensed together in presence of 3% aqueous alkali to get hexamethoxychalcone (**3**) in 92% yield. The chalcone derivative underwent Nazarov's cyclization in presence of trifluoroacetic acid to get the indanone core i.e. compound **4**.

4: Yield: 35%; M.P.: 96- 99C;^{1}H NMR (500 MHz, $CDCl_3$): δ 2.60 (dd, 1H, CH_2), 3.16 (dd, 1H, CH_2), 3.41 (s, 3H, OCH_3), 3.77 (s, 6H, 2 × OCH_3), 3.80 (s, 3H, OCH_3), 3.90 (s, 3H, OCH_3), 3.91 (s, 3H, OCH_3), 4.51 (dd, 1H, 3-CH), 6.29 (s, 2H, aromatic), 7.08 (s, 1H, aromatic); ^{13}C NMR (125 MHz, $CDCl_3$): δ 41.94, 47.10, 56.16, 56.24, 60.17, 60.90, 100.35, 104.26, 132.21, 136.74, 140.13, 144.23, 148.80, 150.44, 153.34, 154.98, 205.24; HRMS-ESI-TOF (MeOH) for $C_{21}H_{24}O_7$ calculated, 389.1600 for $[M + H]^+$ found, 389.1600.

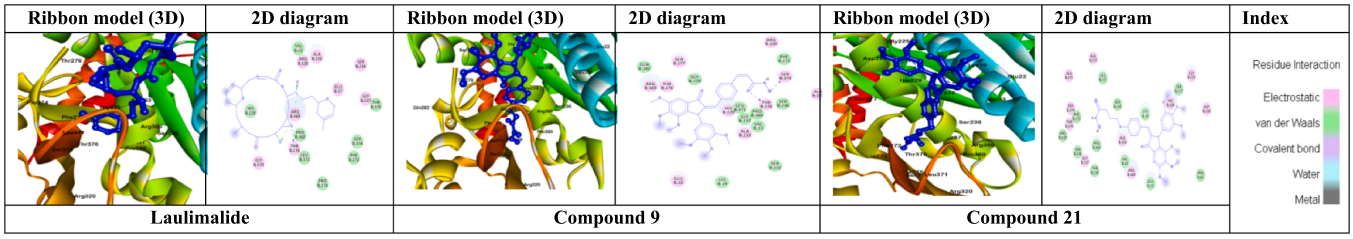

Fig. 5. Docking poses of all the three ligands with beta-tubulin protein.

Table 4
Binding energy, hydrogen bonding, and active binding site residues observed in the *in silico* docking studies of **9** and **21** ligands with selected target (PDB ID:1C3R (HDAC1) and PDB ID: 6THV (HDAC6).

Protein & Ligands	Binding Affinity (Kcal/mol)	H-Bonding	Amino acid residues (4Å)		Protein & Ligands	Binding Affinity (Kcal/mol)	H-Bonding	Amino acid residues (4Å)
PDB ID:1C3R (HDAC1)					PDB ID: 6THV (HDAC6)			
Trichostatin A	-8.5	---	TYR91, PHE141, PRO22, TYR297, LEU265, GLY140, HIS131, HIS132, PHE198, HIS170, GLU92		Tubastatin A	-9.3	---	PHE583, SER531, LEU712, HIS463, PRO464, HIS614, TYR745, PHE643, ASP705, GLY743, HIS574, HIS573, PRO571, CYS584, GLY582
9	-8.3	---	GLY140, TYR297, PHE198, TYR91, PHE200, LYS267, PHE141, HIS170, ASP168, GLY295, HIS131, GLY294, ASP258, HIS132		**9**	-7.3	---	LYS577, ILE622, GLU624, HIS621, ASN617, GLU576, PRO644, SER646, CYS581, HIS574, THR579, ASP578
21	-8.2	---	TYR264, SER266, ASP263, PHE338, PRO22, ASN20, PHE335, TYR297, LEU265, LYS267, ASN269, PHE268, LEU261		**21**	-7.2	---	ASP460, HIS463, ASN457, TRP459, PHE533, ASP527, ASN530, SER531, TYR745, ASP705, ASP612, GLY743, HIS614, HIS573, HIS574, LEU712, PHE643, GLY582, PHE583, ILE532

[Residual amino acids- with blue font, common to all three; with pink font, common to Laulimalide and **9**; with green font, common to Laulimalide and **21**; There are eleven common residual amino acids clearly indicating the same binding pocket occupied by all the three ligands; Trichostatin A non selective, Tubastatin A highly selective HDAC 6 inhibitors].

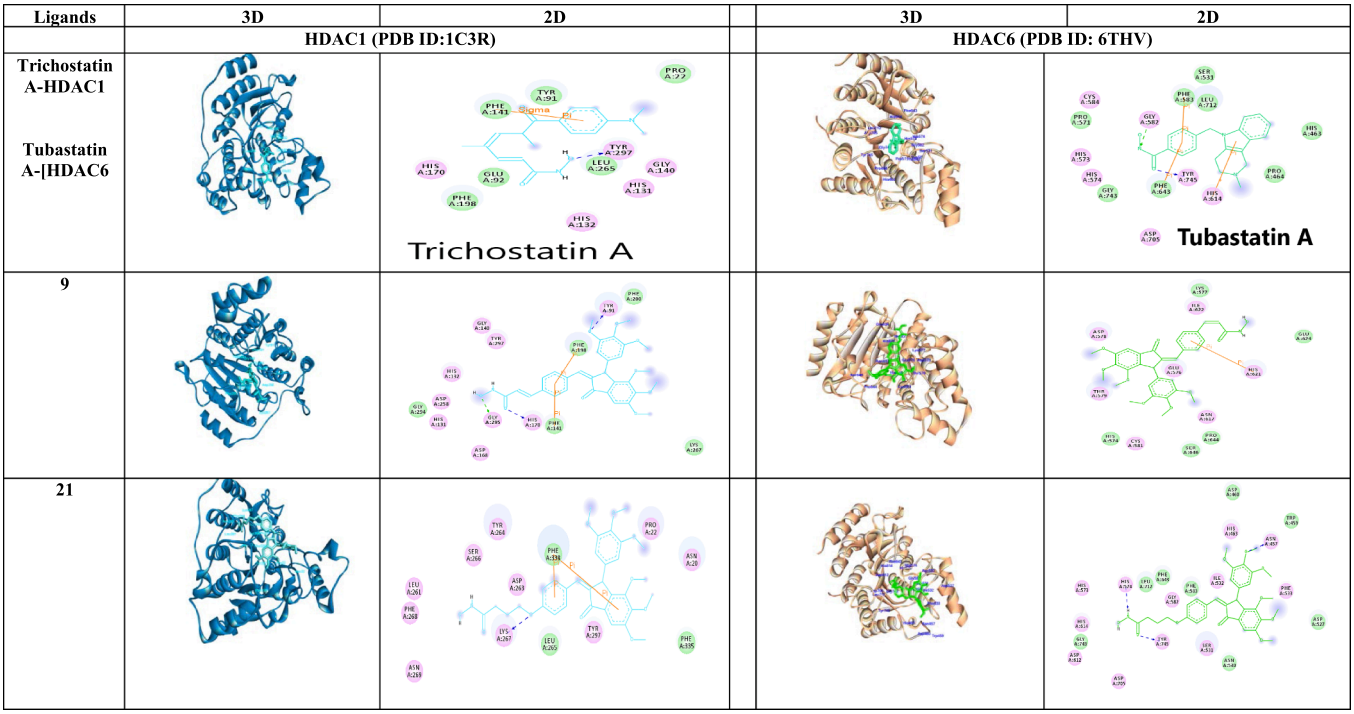

Fig. 6. Docking poses of all the three ligands with HDAC1 and HDAC6 enzymes.

Table 5
Various druggability parameters of Tubastatin A and compd. **21.**

Parameter	Tubastatin A	21	Acceptable range	Parameter	Tubastatin A	21	Acceptable range
Physicochemical properties				**Lipophilicity**			
Molecular formulae	$C_{20}H_{21}N_3O_2$	$C_{32}H_{35}NO_{10}$	–	Log $P_{o/w}$	2.25	3.12	≤5
M.Wt.	335.40	593.62	≤500	**Pharmacokinetics**			
Rotable bonds	4	14	≤10	GI absorption	high	Low	–
H-bond acceptors	3	10	≤10	BBBpermeability	Yes	No	–
H-bond donors	2	2	≤5	P-gp substrate	Yes	Yes	–
Molar Refractivity	100.85	157.18	40–130	CYP1A2 inhibition	Yes	No	–
Sp^3 hybridisation fraction	0.25	0.31	Not less than 0.25	CYP2C9/19 inhibition	No	Yes	–
TPSA	57.50 Å^2	131.01 Å^2	20 Å^2 to 130 Å^2	**Drug likeness**			
Water solubility				Lipinski rule	no violation	Yes, 02 violation	Up to 1 violation
Water solubility	0.96 μg/mL	1.76 μg/mL	soluble	Bioavailability score	0.55	0.17	moderate
Solubility class	Moderate	Moderate	acceptable	**Medicinal chemistry**			
Log S	−3.54	−6.62	>-4	PAINS (False positive)	Yes, 1 alert	No	No

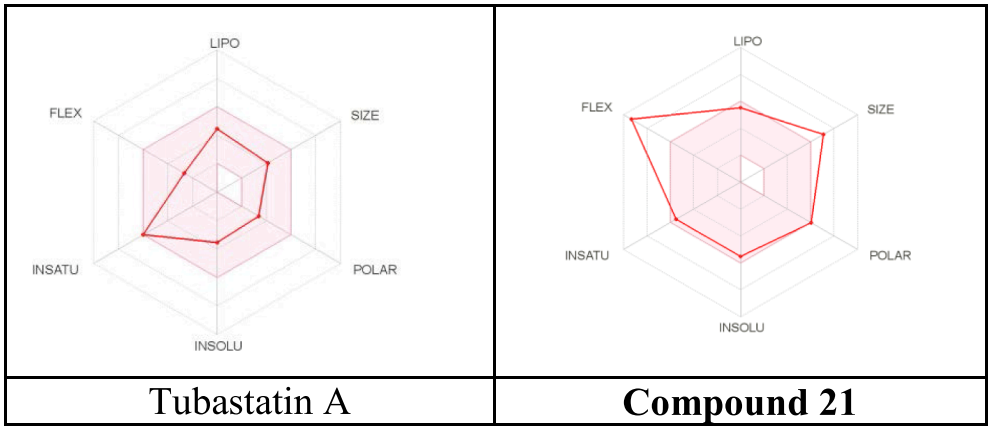

Fig. 7. Two dimensional bioavailability radars of tubastatin A and compound **21.**

Table 6
Effect of compounds **9** and **21** on the pro-inflammatory cytokine levels in the supernatant of peritoneal macrophage cells. Concentrations were expressed in pg/mL (A) TNF-α (B) IL-6.

Compd	LPS (0.1 μg/mL)	Dose (μg/mL)	TNF-α (pg/mL)	TNF-α % inhibition	IL-6 (pg/mL)	IL-6 % inhibition
Normal	–	–	195.90 ± 29.35	NA	1996.53 ± 43.32	NA
Vehicle		–	1219.78 ± 11.13#	–	3013.43 ± 16.41#	–
9		1	1019.21 ± 7.96*	17.28 ± 1.14	2617.2 ± 15.39	13.14 ± 1.1
		10	872.08 ± 16.93*	29.22 ± 1.37	2199.42 ± 40.79*	27.01 ± 1.35
21		1	1180.12 ± 23.07	12.34 ± 1.87	2730.53 ± 42.86	9.38 ± 1.42
		10	1046.79 ± 32.89*	15.04 ± 2.66	2648.31 ± 41.51	12.11 ± 1.37
Dexamethasone		1	581.27 ± 18.24*	52.82 ± 1.48	1792.75 ± 41.11*	40.50 ± 1.88

*P < 0.05; Vehicle vs treatment; #Vehicle vs normal; n = 3; normal without LPS induction, vehicle after.
LPS induction without treatment with compound.

Table 7
Effect of compound **9** as a single acute oral dose at 5, 50, 300 and 1000 mg/kg on body weight, haematological and serum biochemical parameters in Swiss albino mice (Mean ± SE; n = 6; non significant compared to control).

Parameters		Dose of 9 at mg/kg body weight as a single oral dose				
		Control	5 mg/kg	50 mg/kg	300 mg/kg	1000 mg/kg
Body weight (gm)		29.35 ± 0.57	28.17 ± 0.97	28.18 ± 0.80	30.22 ± 0.37	27.43 ± 0.65
Hematological parameters	**Haemoglobin (gm/dL)**	15.66 ± 0.80	17.63 ± 0.65	15.54 ± 0.88	16.77 ± 1.03	16.73 ± 0.84
	RBC (million/mm^3)	7.13 ± 0.40	8.96 ± 0.84	8.82 ± 0.49	8.48 ± 0.62	8.53 ± 0.75
	WBC (1000*/mm^3)	5.29 ± 0.51	5.01 ± 0.41	4.34 ± 0.30	5.75 ± 0.14	4.73 ± 0.27
Liver Function Test	**ALKP (U/L)**	260.10 ± 26.76	221.34 ± 18.22	281.72 ± 44.62	238.88 ± 24.95	277.51 ± 25.58
	SGOT (U/L)	31.51 ± 6.31	28.87 ± 2.20	33.67 ± 1.46	29.93 ± 4.68	33.40 ± 2.65
	SGPT (U/L)	17.01 ± 2.33	16.79 ± 2.13	19.56 ± 1.03	17.95 ± 1.37	22.91 ± 2.00
	Albumin (g/dL)	4.12 ± 0.17	4.34 ± 0.05	4.36 ± 0.11	4.46 ± 0.06	4.53 ± 0.08
	Serum Protein (mg/ml)	5.73 ± 0.21	5.44 ± 0.08	5.64 ± 0.14	5.45 ± 0.15	5.87 ± 0.07
Kidney Function Test	**Creatinine (mg/dL)**	0.76 ± 0.06	0.58 ± 0.05	0.69 ± 0.04	0.64 ± 0.07	0.74 ± 0.05
Lipid profile	**Cholesterol (mg/dL)**	140.17 ± 3.76	162.42 ± 3.08	157.99 ± 5.38	157.14 ± 5.17	157.22 ± 9.94
	Triglycerides (mg/dL)	136.88 ± 3.12	146.79 ± 6.65	129.78 ± 7.59	127.18 ± 2.37	130.21 ± 3.89

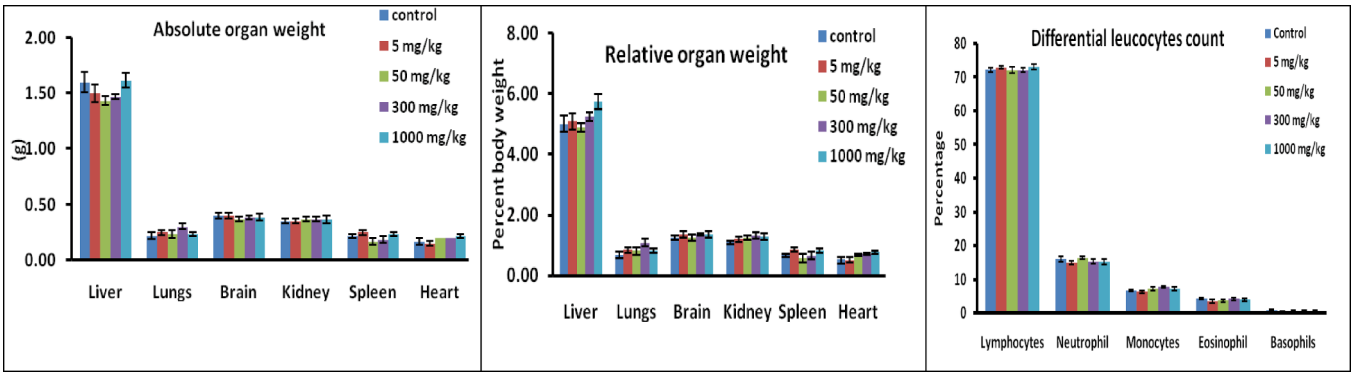

Fig. 8. Effect of **9** as a single acute oral dose at 5, 50, 300 and 1000 mg/kg on a) absolute, b) relative organ weight, and c) on differential leukocyte counts in Swiss albino mice (n = 6, non significant compared to control).

*5.1.2. General procedure for the synthesis of compounds **6, 15, 16** and **29–31**:*

Synthesis of *(E)-Methyl [3-(4-(Z)-4,5,6-trimethoxy-1-oxo-3-(3,4,5-trimethoxyphenyl)-1H-inden-2(3H)ylidene) methyl)phenyl)acrylate (**6**)*.

To a stirred solution of 1.5% KOH in methanol (w/w, 10 mL) at 10 °C, compound **4** (500 mg, 1.29 mmol) was added. To this stirred solution, methyl-4-formylcinnamate (**7**) (270 mg, 1.42 mmol) was added and further stirred at RT for 2 h. On completion, solvent was evaporated, the obtained residue was diluted with water (20 mL), and extracted with ethyl acetate (20 mLx3). The organic layer was washed with water (20 mLx2), dried over anhydrous Na_2SO_4 and evaporated *in-vacuo*. The crude mass was purified through column chromatography over silica gel by eluting with ethyl acetate-hexane to get the desired product **6** as amorphous solid.

6: Yield: 664 mg (92%); M.P.:166–170 °C;^{1}H NMR (500 MHz, $CDCl_3$): δ 3.46 (s, 3H, OCH_3), 3.72 (s, 3H, OCH_3), 3.73 (s, 6H, 2 × OCH_3), 3.80 (s, 3H, OCH_3), 3.91 (s, 3H, OCH_3), 3.94 (s, 3H, OCH_3), 5.31(s, 1H, 3-CH), 6.43(d, 1H, =CH, olefinic, *J*=16 Hz), 6.42(s, 2H, CH, aromatic), 7.22(s, 1H, benzylidene), 7.43(d, 2H, 2 × CH, phenyl ring, *J* = 8 Hz), 7.52(d, 2H, 2 × CH, phenyl ring, *J* = 8.5 Hz), 7.62(d, 1H, olefinic, *J*=16 Hz), 7.67(s, 1H, aromatic); ^{13}C NMR (125 MHz, $CDCl_3$): δ 14.20, 46.24, 51.85, 56.20, 56.32, 60.31, 60.91, 60.96, 101.45, 105.92, 118.91, 127.95, 131.54, 131.93, 133.40, 135.23, 136.27, 136.77, 136.82, 140.87, 140.96, 143.71, 148.92, 149.96, 153.04, 155.01, 167.20, 193.61; HRMS-ESI-TOF (MeOH) for $C_{32}H_{32}O_9$ calculated, 561.2124 for $[M + H]^+$, found, 561.2122.

The procedure of preparation of all these compounds was same except for compounds **29–31** where 3% KOH in MeOH was used.

15: Yield:79%; M.P.:108–110 °C; NMR (500 MHz, $CDCl_3$): δ 1.22–1.26(bt, 3H, CH_3), 2.06–2.10(m, 2H, —CH_2—), 2.46–2.49(bt, 2H, —CH_2CO), 3.48(s, 3H, OCH_3), 3.73(s, 3H, OCH_3), 3.77(s, 3H, 2 × OCH_3), 3.80(s, 3H, OCH_3), 3.98(s, 3H, OCH_3), 4.10–4.11 (bt, 2H,

—OCH_2), 4.12–4.14(bq, 2H, —OCH_2), 5.26(s, 1H, 3-CH), 6.49(s, 1H, CH, aromatic), 6.79(s, 1H, CH, aromatic), 6.80–6.82(d, 2H, 2 × CH, aromatic), 7.28(d, 1H, CH, aromatic), 7.48(d, 1H, CH, aromatic), 7.65(s, 1H, benzylidene), 7.99(s, 1H, CH, aromatic); ^{13}C NMR (125 MHz, $CDCl_3$):δ 14.17, 24.48, 30.64, 31.44, 36.48, 46.34, 56.25, 60.24, 60.46, 60.90, 66.82, 101.43, 114.59, 126.98, 131.96, 132.19, 133.53, 134.48, 136.79, 137.25, 141.17, 139.43, 140.80, 148.48, 149.92, 152.98, 154.84, 160.10, 173.12, 193.85; HRMS-ESI-TOF (MeOH) for $C_{34}H_{38}O_{10}$ calculated, 607.2543 for $[M + H]^+$ found, 607.2543.

16: Yield: 87%; M.P.:178–180 °C; ^{1}H NMR (500 MHz, $CDCl_3$): δ 3.44 (s, 3H, OCH_3), 3.72(s, 6H, 2 × OCH_3), 3.89(s, 3H, OCH_3), 3.91(s, 3H, OCH_3), 3.93(s, 3H, OCH_3), 5.30(s, 1H, 3-CH), 6.39(s, 2H, 2 × CH, aromatic), 7.23(s, 1H, CH, aromatic), 7.54 (d, 2H, 2 × CH, aromatic, J = 8.5 Hz), 7.68(s, 1H, =CH, benzylidene), 7.92(d, 2H, 2 × CH, J = 8.5 Hz); ^{13}C NMR (125 MHz, $CDCl_3$): δ 46.15, 52.26, 56.19, 56.31, 60.29, 60.88, 60.95, 101.46, 105.94, 129.55, 130.79, 131.85, 133.06, 136.68, 136.86, 138.82, 141.05, 141.95, 149.06, 149.98, 153.04, 155.06, 166.46, 193.45; ESI-MS (MeOH): for $C_{30}H_{30}O_9$; 535 $[M + H]^+$;

29: Yield: 92%; M.P.: 206–209 °C; ^{1}H NMR (500 MHz, $CDCl_3$): δ 3.83 (s, 3H, OCH_3), 3.91(s, 3H, —$COOCH_3$), 4.00(s, 2H, CH_2), 6.50(d, 1H, =CH, olefinic, J=16 Hz), 6.96(d, 1H, CH, aromatic), 6.99(s, 1H, =CH, benzylidene), 7.25(s, 1H, CH, aromatic), 7.59 (d, 2H, 2 × CH, aromatic, J = 8.5 Hz), 7.66(d, 2H, 2 × CH, aromatic, J=8.5 Hz), 7.69(d, 1H, =CH, olefinic, J=16 Hz), 7.85(d, 1H, CH, aromatic); ^{13}C NMR (125 MHz, $CDCl_3$): δ 51.84, 55.73, 109.76, 115.39, 118.86, 126.34, 127.71, 128.52, 130.95, 131.53, 135.15, 136.45, 137.47, 143.79, 152.38, 165.41, 167.24, 192.53; HRMS-ESI-TOF (MeOH) for $C_{21}H_{18}O_4$ calculated, 335.1283 for $[M + H]^+$ found, 335.1283.

30: Yield: 88%; M.P.: 197–199 °C; ^{1}H NMR (500 MHz, $CDCl_3$): δ 3.82 (s, 3H, —$COOCH_3$), 3.94(s, 3H, OCH_3), 3.96(s, 2H, CH_2), 3.99(s, 3H, OCH_3), 6.49 (d, 1H, =CH, olefinic, J =16 Hz), 6.97(s, 1H, =CH, benzylidene), 7.32(s, 1H, CH, aromatic), 7.56(s, 1H, CH, aromatic proton), 7.58 (d, 2H, 2 × CH, phenyl ring proton, J=8.5 Hz), 7.65(d, 2H, 2 × CH, aromatic, J=8.5 Hz), 7.68(d, 1H, =CH, olefinic, J = 16 Hz); ^{13}C NMR (125 MHz, $CDCl_3$):δ 33.22, 51.82, 56.18, 56.32, 105.14, 107.18, 118.84, 128.50, 130.91, 131.02, 131.23, 135.13, 136.61, 137.49, 143.77, 144.79, 149.78, 155.63, 167.22, 192.84; Electrospray mass for $C_{22}H_{20}O_5$ (CH_3CN):403$[M + K]^+$.

31: Yield: 91%; M.P.:314–317 °C; ^{1}H NMR (500 MHz, DMSO-d_6):δ 3.82(s, 3H, OCH_3), 3.87(s, 3H, OCH_3), 3.90(s, 3H, OCH_3), 4.01(s, 2H, CH_2), 7.45(s, 1H, =CH, benzylidene), 7.65(s, 1H, CH, aromatic), 7.93(s, 1H, CH, aromatic), 8.03(d, 2H, 2 × CH, aromatic, J=8.5 Hz), 8.10(d, 2H, 2 × CH, aromatic, J=8.5 Hz); ^{13}C NMR (125 MHz, DMSO-d_6): δ31.78, 55.92, 56.24, 56.29, 104.80, 108.40, 129.86, 129.94, 130.82, 131.49, 135.35, 135.85, 138.53, 139.83, 145.75, 149.65, 166.14, 192.06; HRMS-ESI-TOF (MeOH) for $C_{20}H_{18}O_5$ calculated, 339.1232 for $[M + H]^+$, found, 339.1208.

*5.1.3. General procedure for the synthesis of compounds **7, 17, 18, 24**, and **32–34***

Synthesis of *(E)-3-(4-((Z)-(4,5,6-trimethoxy-1-oxo-3-(3,4,5-trimethoxyphenyl)-1H-inden-2(3H)-ylidene) methyl) phenyl-prop-2-enoic acid (7)*.

To a stirred solution of 3% KOH in MeOH-H_2O (9:1), ester **6** (500 mg, 0.89 mmol) was taken and further stirred at50°C for 2 h. On completion, the reaction mixture was acidified with 5% dil. HCl (10 mL) and extracted with ethyl acetate. The ethyl acetate was washed with water (20 mLx2), dehydrated with anhydrous sodium sulphate and evaporated to dryness to get a residue. The residue was recrystallized from chloroform-hexane to get corresponding acid **7** as amorphous solid.

7: Yield: 434 mg (89%); M.P.: 238–241 °C; ^{1}H NMR (500 MHz, $CDCl_3$): δ3.46(s, 3H, OCH_3), 3.73 (s, 9H, 3 × OCH_3), 3.91(s, 3H, OCH_3), 3.93(s, 3H, OCH_3), 5.31(s, 1H, 3-CH), 6.44(d, 1H, =CH, olefinic, J=16 Hz), 6.43(s, 2H, CH, aromatic), 7.25(s, 1H, benzylidene), 7.45(d, 2H, J=8.5 Hz, aromatic), 7.54(d, 2H, aromatic, J = 8.5 Hz), 7.67(s, 1H, CH, aromatic), 7.71(d, 1H, =CH, olefinic, J =16 Hz); ^{13}C NMR (125 MHz, $CDCl_3$):δ 46.25, 56.24, 56.31, 60.30, 60.89, 60.94, 101.50, 106.05, 118.32, 128.20, 131.54, 131.91, 133.29, 134.85, 136.71, 136.73, 136.96, 140.97, 141.13, 145.75, 148.98, 149.97, 153.08, 155.05, 171.23, 193.57; HRMS-ESI-TOF (MeOH) for $C_{31}H_{30}O_9$ calculated, 545.1811 for $[M-H]^-$ found, 545.1819.

17: Yield: 83%; M.P.: 163–165 °C; ^{1}H NMR (500 MHz, $CDCl_3$):δ 2.02–2.15(m, 2H, —CH_2—), 2.53–2.55(bt, 2H, —CH_2CO), 3.46(s, 3H, OCH_3), 3.74(s, 3H, OCH_3), 3.85(s, 3H, 2 × OCH_3), 3.89(S, 3H, OCH_3), 3.99(S, 3H, OCH_3), 4.00(bt, 2H, OCH_2), 5.26(s, 1H, 3-CH), 6.48(s, 2H, 2 × CH, aromatic), 6.96(d, 2H, 2 × CH, aromatic,J=8.5 Hz), 7.47(d, 2H, 2 × CH, aromatic, J=8.5 Hz), 7.23(s, 1H, =CH, benzylidene), 7.65(s, 1H, CH, aromatic); ^{13}C NMR (125 MHz, $CDCl_3$):δ 14.19, 21.05, 24.27, 30.29, 46.37, 56.10, 56.29, 60.46, 60.95, 61.70, 66.63, 72.24, 101.48, 105.86, 114.39, 127.01, 132.18, 133.58, 134.65, 136.87, 137.22, 148.52, 149.93, 153.32, 160.06, 177.74, 194.04; HRMS-ESI-TOF (MeOH) for $C_{32}H_{34}O_{10}$ calculated, 579.2230 for $[M + H]^+$ found, 579.2231.

18: Yield: 81%; M.P.: 229–231 °C; ^{1}H NMR (500 MHz, $CDCl_3$): δ3.45 (s, 3H, OCH_3), 3.73(s, 6H, 2 × OCH_3), 3.73((s, 3H, OCH_3), 3.91(s, 3H, OCH_3), 3.95(s, 3H, OCH_3), 5.32(s, 1H, 3-CH), 6.39(s, 2H, 2 × CH, aromatic), 7.25(s, 1H, CH, aromatic), 7.58(d, 2H, 2 × CH, J=8.0 Hz), 7.71 (s, 1H, =CH, benzylidene), 8.00(d, 2H, 2 × CH, aromatic, J=8.5 Hz); ^{13}C NMR (125 MHz, $CDCl_3$):δ 41.40, 51.45, 51.58, 55.56, 56.17, 56.23, 96.72, 101.13, 121.66, 124.56, 125.27, 126.00, 127.08, 128.16, 131.94, 132.09, 134.91, 136.33, 137.58, 144.37, 145.23, 148.31, 150.34, 165.01, 188.70; HRMS-ESI-TOF (MeOH) for $C_{29}H_{28}O_9$ calculated, 519.1655 for $[M-H]^-$ found, 519.1673.

24: Yield: 72%; oil; ^{1}H NMR (500 MHz, $CDCl_3$): δ2.81–2.92(dd, 1H, CH_2, $J_{ab,}$ benzylic), 2.93–2.94(dd, 1H, CH_2, benzylic), 3.34(s, 3H, OCH_3), 3.40(bm, 1H, 3-CH), 3.59(s, 3H, 2 × OCH_3), 3.78(s, 3H, OCH_3), 3.89(s, 3H, OCH_3), 3.95(s, 3H, OCH_3), 4.12(d, 1H, 3-CH), 5.86(s, 2H, 2 × CH, aromatic), 7.11(s, 1H, CH, aromatic), 7.34(d, 2 × CH, aromatic, J=8.5 Hz), 8.02(d, 2 × CH, aromatic, J=8.0 Hz); ^{13}C NMR (125 MHz, $CDCl_3$):δ 37.63, 47.72, 55.98, 56.27, 59.26, 60.12, 60.87, 100.61, 104.06, 127.68, 129.62, 130.41, 131.35, 136.60, 139.51, 142.68, 145.72, 149.20, 150.48, 153.14, 155.23, 171.16, 205.91; ESI-MS (MeOH) for $C_{29}H_{30}O_9$: 523 $[M + H]^+$, 545 $[M + Na]^+$, Negative mode: 521 $[M-H]^-$;

32: Yield: 89%; M.P.: 301–303 °C (Blackens); ^{1}H NMR (500 MHz, DMSO-d_6): δ 3.90(s, 3H, OCH_3), 4.10(s, 2H, CH_2), 6.62–6.65(d, 1H, =CH, olefinic,J=16 Hz,), 7.04(d, 1H, CH, aromatic, J=8.5 Hz), 7.20(s, 1H, CH, aromatic), 7.46(s, 1H, =CH, benzylidene), 7.64(d, 1H, =CH, olefinic, J= 16 Hz,), 7.73(d, 2H, 2 × CH, aromatic, J=8.5 Hz), 7.79(d, 2H, 2 × CH, aromatic, J=8.5 Hz), 7.81(d, 1H, CH, aromatic, J = 8.5 Hz); ^{13}C NMR (125 MHz, DMSO-d_6):δ 32.09, 55.84, 110.19, 115.52, 120.36, 125.56, 128.74, 130.49, 130.66, 130.99, 135.18, 136.71, 143.04, 153.04, 165.05, 167.51, 191.53; HRMS-ESI-TOF (MeOH) for $C_{20}H_{16}O_4$ calculated, 321.1126 for $[M + H]^+$ found, 321.1121.

33: Yield: 86%; M.P.:196–199 °C; ^{1}H NMR (500 MHz, DMSO-d_6): δ 3.83(s, 3H, OCH_3), 3.90(s, 3H, OCH_3), 4.01(s, 2H, CH_2), 6.63(d, 1H, =CH, olefinic, J=15.5 Hz), 7.14(s, 1H, =CH, benzylidene), 7.22(s, 1H, CH, aromatic), 7.43(s, 1H, CH, aromatic), 7.63(d, 1H, =CH, olefinic, J = 15.5 Hz), 7.72(d, 2H, 2 × CH, aromatic, J=7.5 Hz), 8.15(d, 2H, 2 × CH, aromatic, J=7.0 Hz); ^{13}C NMR (125 MHz, DMSO-d_6):δ 31.64, 55.65, 56.00, 104.58, 108.04, 120.33, 127.77, 128.69, 130.17, 130.88, 131.28, 135.09, 136.88, 142.97, 145.17, 149.37, 155.41, 167.49, 191.73; ESI-MS (MeOH) for $C_{21}H_{18}O_5$; 351 $[M + H]^+$, 389 $[M + K]^+$; Negative mode: 349 $[M-H]^-$;

34: Yield: 87%; M.P.:279–282 °C (Blackens); ^{1}H NMR (500 MHz, pyridine-d_5):δ 3.32(s, 3H, OCH_3), 3.38(s, 3H, OCH_3), 3.44(s, 2H, CH_2), 6.50(s, 1H, =CH, benzylidene), 6.75(s, 1H, CH, aromatic), 7.12(s, 1H, CH, aromatic), 7.37(d, 2H, 2 × CH, aromatic, J=7.5 Hz), 8.05(d, 2H, 2 × CH, aromatic, J = 7.5 Hz); ^{13}C NMR (125 MHz, pyridine-d_5):δ 32.74, 56.34, 56.68, 106.09, 108.71, 123.62, 123.86, 124.05, 124.25, 131.24, 131.66, 139.01, 140.43, 146.08, 150.96, 156.92, 192.97; Electrospray mass for $C_{19}H_{16}O_5$ (MeOH): 325$[M + H]^+$, 347$[M + Na]^+$, 363$[M + K]^+$, Negative mode: 323$[M-H]^-$; HRMS-ESI-TOF (MeOH) for $C_{19}H_{16}O_5$

calculated, 325.1076 for $[M + H]^+$found, 325.0964.

5.1.4. General procedure for the synthesis of compounds 8, 19, 20, 25, 35–37 and 41

Synthesis of (E)-N-((tetrahydro-2H-pyran-2-yl)oxy)--*3-(4-((Z)-(4,5,6-trimethoxy-1-oxo-3-(3,4,5-trimethoxyphenyl)-1H-inden-2(3H)-ylidene) methyl) phenyl-prop-2-enamide (8)*.

To a stirred solution of dry dichloromethane (15 mL), acid **7** (500 mg, 0.91 mmol) was added. To this *N*-methyl morpholine (0.6 mL, 5.46 mmol), DMAP (12 mg, 0.11 mmol) and cyanuric chloride (80 mg, 0.43 mmol) were added. Now *O*-THP-hydroxylamine [*O*-tetrahydro-2H-pyran-2-yl) hydroxylamine] was added to this and further stirred at RT for an hour. On completion, water (20 mL) was added to this and reaction mixture was extracted with chloroform (20mLx2), organic layer was washed with water (20mLx2) and dehydrated with anhydrous sodium sulphate. The residue thus obtained was charged on a silica gel column (100–200 mesh) and eluted with hexane–ethyl acetate to get the desired product at 5–10% EA-Hexane, which on recrystallization from hexane afforded compound **8** as an amorphous solid.

8: Yield: 360 mg (61%); M.P.: 167–170 °C; ^{1}H NMR (500 MHz, $CDCl_3$): δ1.60–1.1.89 (m, 6H, 3 × CH_2), 3.47(s, 3H, OCH_3), 3.65 (t, 2H, OCH_2), 3.75(s, 9H, 3 × OCH_3), 3.82(s, 3H, OCH_3), 3.94(s, 3H, OCH_3), 4.11(t, 1H, 3-CH), 5.30(s, 1H, 3-CH), 6.43(bd, 3H, ═CH & 2 × CH, olefinic and aromatic), 7.23(s, 1H, CH, aromatic), 7.40(d, 2H, 2 × CH, aromatic, *J*=7.5 Hz), 7.50(d, 2H, 2 × CH, aromatic, *J* = 8.0 Hz), 7.66(bs, 2H, olefinic and benzylidene); ^{13}C NMR (125 MHz, $CDCl_3$): δ14.20, 18.69, 21.06, 23.39, 24.97, 28.07, 29.70, 33.26, 46.25, 50.87, 56.22, 56.31, 60.30, 60.42, 60.91, 60.95, 62.75, 67.44, 98.47, 101.45, 105.97, 127.84, 131.51, 131.53, 131.96, 133.46, 135.53, 135.99, 136.83, 140.72, 140.95, 148.90, 149.96, 153.04, 155.02, 193.60; HRMS-ESI-TOF (MeOH) for $C_{36}H_{39}NO_{10}$ calculated, 646.2652 for $[M + H]^+$ found, 646.2638.

19: Yield: 59%; M.P.: 103–105 °C; ^{1}H NMR (500 MHz, $CDCl_3$): δ 1.56–1.78(m, 6H, CH_2), 2.11–2.17(m, 2H, —CH_2—), 2.30–2.35(bt, 2H, —CH_2CO), 3.57(t, 2H, OCH_2), 3.48(s, 3H, OCH_3), 3.77–3.78(s, 3H, OCH_3), 3.80(s, 6H, 2 × OCH_3), 3.89(s, 3H, OCH_3), 3.99(s, 3H, OCH_3), 4.01(t, 2H, OCH_2), 4.93(t, 2H, OCH_2), 5.26(s, 1H, 3-CH), 6.49(s, 2H, 2 × CH, aromatic), 6.78(d, 2H, 2 × CH, aromatic, *J*=9.0 Hz), 7.54(d, 2H, 2 × CH, aromatic, *J*=9.0 Hz), 7.23(s, 1H, ═CH, benzylidene), 8.13(s, 1H, CH, aromatic); ^{13}C NMR (125 MHz, $CDCl_3$): δ18.56, 24.95, 25.22, 27.97, 29.66, 46.39, 56.29, 60.28, 60.90, 62.58, 66.76, 93.26, 100.94, 101.44, 102.47, 106.03, 114.42, 114.59, 114.77, 127.09, 128.92, 132.01, 132.23, 133.26, 134.46, 136.77, 136.89, 137.32, 140.32, 148.49, 149.99, 153.00, 154.86, 170.15, 193.85; HRMS-ESI-TOF (MeOH) for $C_{37}H_{43}NO_{11}$ calculated, 678.2914 for $[M + H]^+$ found, 678.2914.

20: Yield: 52%; light orange amorphous solid; M.P.: 110–112 °C; ^{1}H NMR (500 MHz, $CDCl_3$): δ1.20–1.81(bt, 6H, 2 × CH_2), 3.43(s, 3H, OCH_3), 3.70(s, 3H, OCH_3), 3.74 (s, 3H, OCH_3), 3.89(s, 6H, 2 × OCH_3), 3.91(s, 3H, OCH_3), 4.06–4.11(bt, 2H, —OCH_2), 5.03(s, 1H, 3-CH), 5.25 (t, 3H, O-CH-O), 6.37(s, 2H, 2 × CH, aryl proton), 7.50(d, 2H, 2 × CH, *J*=8.0 Hz), 7.64(d, 2H, 2 × CH, *J*=7.5 Hz), 7.20(s, 1H, CH, aromatic proton), 7.24(s, 1H, ═CH, benzylidine proton), 8.90(s, 1H, —NH); ^{13}C NMR (125 MHz, $CDCl_3$): δ 14.19, 18.61, 21.05, 25.01, 28.05, 46.15, 56.22, 56.30, 60.40, 60.95, 62.70, 101.44, 102.75, 105.89, 127.18, 131.03, 131.80, 132.29, 132.89, 136.65, 136.68, 136.85, 138.01, 141.00, 149.04, 149.97, 153.07, 155.06, 171.18, 193.45; HRMS-ESI-TOF (MeOH) for $C_{34}H_{37}NO_{10}$ calculated, 619.2417 for $[M + H]^+$, found, 642.2315.

25: Yield: 81%; brown amorphous solid, M.P.: 108–110 °C; ^{1}H NMR (500 MHz, $CDCl_3$): δ1.60–1.87(bm, 6H, 3 × CH_2), 2.79(dd, 1H, CH_2, benzylic proton), 2.87(dd, 1H, CH_2, benzylic proton), 3.34(s, 3H, OCH_3), 3.49(bm, 1H, 3-CH), 3.59(s, 3H, 2 × OCH_3), 3.76(s, 3H, OCH_3), 3.89(s, 3H, OCH_3), 3.93(s, 3H, OCH_3), 4.08–4.13(bm, 3H, 3-CH & OCH_2), 5.05(t, 1H, O-CH-O), 5.84(s, 2H, 2 × CH, aryl proton), 7.08 (s, 1H, CH, aromatic proton), 7.28(d, 2 × CH, phenyl ring proton, *J*=8.0 Hz), 7.67(d, 2 × CH, phenyl ring proton, *J*=8.0 Hz); ^{13}C NMR (125 MHz, $CDCl_3$): δ 20.33, 25.03, 28.08, 47.61, 56.26, 59.32, 60.11, 60.41, 60.96, 62.76, 100.53, 102.78, 104.09, 127.39, 128.90, 129.78, 130.39, 131.39, 136.58, 139.55, 139.58, 142.64, 143.70, 149.15, 150.47, 153.13, 155.20, 171.19, 205.89; HRMS- ESI-TOF (MeOH) for $C_{34}H_{39}NO_{10}$ calculated, 621.2573 for $[M + Na]^+$, found, 644.2471.

35: Yield: 72%;M.P.:146–149 °C; ^{1}H NMR (500 MHz, DMSO-d_6): δ 1.64–1.73(bm, 6H, 3 × CH_2), 3.50–3.62(bs, 2H, CH_2), 3.84(s, 3H, OCH_3), 3.89–4.09(bs, 3H, OCH_2 & OCHO—), 6.62(s, 1H, CH, benzylidene), 7.19(s, 1H, CH, aromatic), 7.37(d, 1H, CH, aromatic), 7.45–7.53 (d, 1H, CH, aromatic), 7.63(d, 1H, ═CH, olefinic, *J*=15 Hz), 7.73(bd, 4H, 4 × CH, aromatic, *J*=6.5 Hz), 7.79(d, 1H, ═CH, olefinic, *J*=15.5 Hz), 11.30(s, 1H, —NH); ^{13}C NMR (125 MHz, DMSO-d_6): δ19.22, 24.27, 28.29, 56.00, 61.03, 78.94, 100.70, 109.79, 155.06, 119.49, 125.12, 126.74, 127.74, 129.15, 130.28, 131.00, 134.12, 135.85, 136.09, 138.26, 152.56, 165.58, 191.09; HRMS-ESI-TOF (MeOH) for $C_{25}H_{25}NO_5$ calculated, 420.1810 for $[M + H]^+$ found result, 420.1800.

36: Yield: 73%; Green amorphous solid;M.P.:255–259 °C; ^{1}H NMR (500 MHz, $CDCl_3$): δ 1.76–2.04(bm, 6H, 2 × CH_2, pyran ring proton), 3.59–3.67(s, 2H, CH_2), 3.91(s, 3H, OCH_3), 3.99(s, 3H, OCH_3), 5.18 (t, 1H, —OCHO-), 6.77(s, 1H, ═CH, benzylidene proton), 6.94(d, 1H, ═CH, olefinic proton, *J*=15.5 Hz), 7.33(s, 1H, CH, aromatic proton), 7.50(d, 2H, 2 × CH, phenyl ring proton, *J* = 6.5 Hz), 7.63(s, 1H, CH, aromatic proton), 7.58(d, 2H, 2 × CH, phenyl ring proton, *J*=8.0 Hz),7.67(d, 1H, ═CH, olefinic proton, *J*=16.5 Hz); ^{13}C NMR (125 MHz, $CDCl_3$): δ22.76, 25.52, 28.89, 37.47, 56.18, 56.31, 63.25, 100.82, 104.30, 105.17, 106.86, 107.21, 115.91, 118.47, 123.95, 127.41, 128.24, 131.38, 136.75, 141.43, 144.84, 155.45, 166.52, 192.98; ESI-MS (MeOH): for $C_{26}H_{27}NO_6$;450 $[M + H]^+$, 488$[M + K]^+$.

37: Yield: 72%; light green amorphous solid; M.P.:163–165 °C; ^{1}H NMR (500 MHz, DMSO-d_6): δ 1.27–1.74(bm, 6H, 2 × CH_2, pyran ring proton), 3.82(s, 3H, OCH_3), 3.87(s, 3H, OCH_3), 3.90(s, 3H, OCH_3), 3.91 (s, 2H, CH_2), 4.04(t, 2H, OCH_2), 5.02(t, 1H, —OCHO-), 7.14(s, 1H, ═CH, benzylidene proton), 7.46(s, 1H, CH, aromatic proton), 7.88(d, 2H, 2 × CH, phenyl ring proton, *J*=8.5 Hz), 7.95(s, 1H, CH, aromatic proton), 8.13(d, 2H, 2 × CH, phenyl ring proton, *J* = 8.0 Hz); ^{13}C NMR (125 MHz, DMSO-d_6): δ21.72, 24.71, 27.88, 34.68, 55.61, 56.03, 61.42, 101.05, 104.61, 108.05, 127.72, 130.54, 132.51, 135.46, 137.65, 138.09, 144.21, 145.29, 149.39, 155.49, 162.29, 191.67; HRMS-ESI-TOF (MeOH) for $C_{24}H_{25}NO_6$ calculated, 422.1603 for $[M-H]^-$ found, 422.1603.

5.1.5. General procedure for the synthesis of compounds 9, 21, 22, 26, and 38–40

Synthesis of (E)-N-Hydroxy-3-(4-((Z)-(4,5,6-trimethoxy-1-oxo-3-(3,4,5-trimethoxyphenyl)-1H-inden-2(3H)-ylidene)methyl) phenyl-prop-2-enamide(9).

In a stirred solution of dry methanol (20 mL), protected hydroxylamine derivative **8** (500 mg, 0.77 mmol) was added. To this p-toluene sulphonic acid (p-TSA, 10 mg, 0.06 mmol) was added and further stirred at RT for 30 min. On completion, solvent was evaporated and water (20 mL) was added to this. It was extracted with ethyl acetate (20 mLx3), washed with water (20 mLx2), dehydrate with anhydrous sodium sulphate and dried in-vacuo. The crude mass was charged on a silica gel (100–200 mesh) column and eluted with ethyl acetate-hexane to get the desired compound at 60% ethyl acetate-hexane to get yellowish green amorphous hydroxamic acid derivative **9**.

9: Yield: 313 mg (72%) yellow solid; M.P.: 107–110 °C; ^{1}H NMR (500 MHz, $CDCl_3$): δ2.03(bs, 1H, —OH), 3.47(s, 3H, OCH_3), 3.75(s, 9H, 3 × OCH_3), 3.84(s, 3H, OCH_3), 3.92(s, 3H, OCH_3), 5.27 (s, 1H, 3-CH), 6.40(bd, 3H, ═CH, 2 × CH, olefinic & aryl proton, *J*=16 Hz), 7.24(d, 1H, ═CH, olefinic proton, *J*=15.5 Hz), 7.29(d, 2H, 2 × CH, phenyl ring proton, *J*=6.0 Hz), 7.41(d, 2H, 2 × CH, phenyl ring proton, *J*=6.5 Hz), 7.25(s, 1H, benzylidine proton), 7.62 (s, 1H, CH, aromatic proton); ^{13}C NMR (125 MHz, $CDCl_3$): δ46.26, 56.24, 56.31, 60.30, 60.92, 60.97, 101.47, 106.03, 127.73, 131.51, 131.91, 133.52, 135.83, 136.70,

140.67, 140.91, 148.94, 149.94, 153.01, 155.04, 193.63; HRMS-ESI-TOF (MeOH) for $C_{31}H_{31}NO_9$ calculated, 560.1920 for $[M-H]^-$ found, 560.1939.

21: Yield: 69%; red coloured solid; M.P.: 78–80 °C; ^{1}H NMR (500 MHz, $CDCl_3$): δ2.03–2.07(bm, 2H, CH_2), 2.30–2.34(bt, 2H, —CH_2CO-), 3.47(s, 3H, OCH_3), 3.73(s, 3H, OCH_3), 3.87(s, 3H, 2 × OCH_3), 3.99(s, 3H, OCH_3), 4.12(t, 2H, OCH_2), 5.26(s, 1H, 3-CH), 6.47(s, 2H, 2 × CH, aryl aromatic proton), 6.73(d, 2H, 2 × CH, *J*=8.5 Hz, phenyl proton), 7.24(s, 1H, =CH, benzylidene proton), 7.43(d, 2H, 2 × CH, phenyl proton, *J*=8.5 Hz), 7.65(s, 1H, CH, aromatic proton); ^{13}C NMR (125 MHz, $CDCl_3$): δ22.68, 24.79, 29.68, 46.38, 54.91, 56.22, 56.29, 60.26, 60.92, 66.70, 101.47, 106.15, 114.34, 127.14, 132.25, 133.14, 133.50, 134.55, 136.63, 136.85, 137.58, 140.75, 148.56, 150.00, 152.91, 154.90, 159.85, 193.81; HRMS-ESI-TOF (MeOH) for $C_{32}H_{35}NO_{10}$ calculated, 594.2339 for $[M + H]^+$ found, 594.2331.

22: Yield: 63%; M.P.:138–142 °C; ^{1}H NMR (500 MHz, $CDCl_3$): δ 3.44 (s, 3H, OCH_3), 3.72(s, 3H, OCH_3), 3.90 (s, 3H, OCH_3), 3.93(s, 6H, 2 × OCH_3), 3.91(s, 3H, OCH_3), 5.03(s, 1H, 3-CH), 6.39(s, 2H, 2 × CH, aryl proton), 7.20(s, 1H, CH, aromatic proton), 7.54(d, 2H, 2 × CH, *J*=8.0 Hz), 7.69(s, 1H, =CH, benzylidine proton), 7.93(d, 2H, 2 × CH, *J*=8.0 Hz), 8.90(s, 1H, —NH); ^{13}C NMR (125 MHz, $CDCl_3$): δ46.16, 52.28, 56.23, 56.32, 60.30, 60.89, 60.96, 101.46, 105.91, 129.43, 130.36, 130.71, 131.85, 133.09, 136.69, 136.83, 138.82, 141.06, 141.93, 149.06, 149.98, 153.04, 155.06, 166.47, 193.46; HRMS-ESI-TOF (MeOH) for $C_{29}H_{29}NO_9$ calculated, 535.1842 for $[M + H]^+$ found, 536.1920.

26: Yield: 74%; M.P.: 107–110 °C; ^{1}H NMR (500 MHz, $CDCl_3$): δ 2.78–2.89(dd, 1H, CH_2, $J_{ab,}$ benzylic proton), 2.90–2.92(dd, 1H, CH_2, J_{ba} benzylic proton), 3.34(s, 3H, OCH_3), 3.40(bm, 1H, 3-CH), 3.57 (s, 3H, 2 × OCH_3), 3.71(s, 3H, OCH_3), 3.89(s, 3H, OCH_3), 3.93(s, 3H, OCH_3), 4.08(d, 1H, 3-CH), 5.58(s, 2H, 2 × CH, aryl proton), 7.09(s, 1H, CH, aromatic proton), 7.28(d, 2 × CH, phenyl ring proton, *J*=7.5 Hz), 7.65(d, 2 × CH, phenyl ring proton, *J*=7.0 Hz); ^{13}C NMR (125 MHz, $CDCl_3$): δ33.83, 37.22, 47.79, 56.10, 56.27, 59.27, 60.11, 60.88, 60.90, 100.60, 104.20, 127.05, 129.01, 129.88, 131.55, 136.61, 139.56, 142.64, 143.97, 149.21, 150.44, 153.11, 155.22, 166.46, 205.88; HRMS-ESI-TOF (MeOH) for $C_{29}H_{31}NO_9$ calculated, 537.1998 for $[M + Na]^+$, found, 538.2077.

38: Yield: 78%; Pale yellow amorphous solid; M.P.: 91–94 °C; ^{1}H NMR (500 MHz, DMSO-d_6): δ3.89 (s, 3H, OCH_3), 4.10(s, 2H, CH_2), 6.55 (d, 1H, =CH, olefinic proton, *J*=16 Hz), 7.04(d, 1H, CH, aromatic proton, *J* = 8.5 Hz), 7.19(s, 1H, CH, aromatic proton), 7.45(s, 1H, =CH, benzylidine proton), 7.51(d, 1H, =CH, olefinic proton, *J*=16 Hz), 7.68 (d, 1H, CH, aromatic proton, *J*=8.0 Hz). 7.73(d, 2H, 2 × CH, phenyl ring proton, *J* = 8.5 Hz), 7.80(d, 2H, 2 × CH, phenyl ring proton, *J*=8.5 Hz), 9.12(s, 1H, —NH); ^{13}C NMR (125 MHz, DMSO-d_6): δ 32.10, 55.86, 110.21, 115.51, 120.27, 125.63, 130.53, 130.73, 131.13, 133.91, 136.37, 153.03, 162.56, 162.7, 165.04, 191.56; HRMS-ESI-TOF (MeOH) for $C_{20}H_{17}NO_4$ calculated, 336.1235 for $[M + H]^+$, found, 3361232.

39: Yield: 52 %; oil; ^{1}H NMR (500 MHz, $CDCl_3$): δ3.66(s, 2H, CH_2), 3.75(s, 3H, OCH_3), 3.85(s, 3H, OCH_3), 6.52(d, 1H, =CH, olefinic proton), 6.61(s, 1H, =CH, benzylidene proton), 7.04(s, 1H, CH, aromatic proton), 7.13 (s, 1H, CH, aromatic proton), 7.66(bm, 5H, 4 × CH, =CH), 8.22(s, 1H, —NH); ^{13}C NMR (125 MHz, $CDCl_3$): δ47.20, 51.82, 56.05, 63.81, 70.51, 98.38, 102.53, 117.59, 123.49, 127.59, 132.72, 141.52, 149.48, 155.61, 160.73, 168.27, 182.72, 188.42, 200.53; Electrospray mass for $C_{21}H_{19}NO_5$ (MeOH): Positive mode, 388$[M + Na]^+$.

40: Yield: 74%; Yellow amorphous solid; M.P.: 255–259 °C (Blackens); ^{1}H NMR (500 MHz, DMSO-d_6): δ3.83(s, 3H, OCH_3), 3.90(s, 3H, OCH_3), 4.02(s, 2H, CH_2), 7.21(s, 1H, =CH, benzylidene proton), 7.42(s, 1H, CH, aromatic proton), 7.49(d, 2H, 2 × CH, phenyl ring proton, *J* = 8.0 Hz), 7.71(d, 2H, 2 × CH, phenyl ring proton, *J* = 7.5 Hz), 7.85(s, 1H, CH, aromatic proton), 8.45(s, 1H, —NH); ^{13}C NMR (125 MHz, DMSO-d_6):δ 32.31, 56.37, 56.52, 79.59, 104.91, 108.56, 114.34, 122.86, 130.13, 131.09, 133.12, 144.80, 149.61, 151.29, 155.12, 163.00, 192.35; HRMS-ESI-TOF (MeOH) for $C_{19}H_{17}NO_5$ calculated, 338.1028 for $[M-H]^-$ found, 338.1067.

5.1.6. General procedure for the synthesis of compounds **11** and **42**, **43**, **46**, and **47**

Synthesis of (E)-N-benzyloxy-*3-(4-((Z)-(4,5,6-trimethoxy-1-oxo-3-(3,4,5-trimethoxyphenyl)-1H-inden-2(3H)-ylidene) methyl) phenyl-prop-2-enamide(**11**)*.

To a stirred solution of dry DMF (20 mL) acid **7** (500 mg, 0.91 mmol) was taken. To this stirred solution triethyl amine (0.5 mL, 363 mg, 3.59 mmol), EDC-HCl (190 mg, 1.0 mmol), and HOBt (135 mg, 1.0 mmol) were added and stirred at 60 °C for 15 min. Now *O*-benzylhydroxylamine hydrochloride (NH_2OBn-HCl, 160 mg, 1.0 mmol) was added to this and reaction mixture was further stirred at 60 °C for an hour. On completion water (30 mL) was added to it and reaction mixture was extracted with ethyl acetate (20 mLx3). Combined organic fraction was washed with water (20 mL), dehydrated with anhydrous sodium sulphate and evaporated. The residue thus obtained was charged on silica gel (100–200 mesh) column and eluted with hexane–ethyl acetate to get the desired product **11** as amorphous solid.

11: Yield: 60%; M.P.: 109–113 °C; ^{1}H NMR (500 MHz, $CDCl_3$): δ 3.47 (s, 3H, OCH_3), 3.78(s, 6H, 2 × OCH_3), 3.84(s, 3H, OCH_3), 3.89(s, 3H, OCH_3), 3.91(s, 3H, OCH_3), 4.96(s, 2H, -OCH_2Bn), 5.30(s, 1H, 3-CH), 6.41(s, 3H, 2 × CH, =CH, aryl proton + olefinic proton), 7.23(s, 1H, CH, aromatic proton), 3.35–7.39(bm, 5H, 5 × CH, benzyl aromatic proton), 7.41(d, 2H, 2 × CH, phenyl ring proton, *J*=8.0 Hz), 7.49(d, 2H, 2 × CH, phenyl ring proton, *J*=8.5 Hz), 7.64(d, 1H, =CH, olefinic proton, *J*=15.5 Hz); ^{13}C NMR (125 MHz, $CDCl_3$): δ46.24, 55.91, 56.22, 56.31, 60.18, 60.30, 60.89, 60.95, 101.46, 105.36, 106.01, 114.07, 125.03, 127.87, 128.59, 128.95, 129.61, 131.50, 131.61, 131.95, 133.45, 135.21, 136.86, 140.76, 140.93, 148.91, 149.96, 151.01, 153.04, 155.03, 193.59; ESI-MS (MeOH) for $C_{38}H_{37}NO_9$; 652 $[M + H]^+$, 690 $[M + K]^+$; Negative mode: 650 $[M-H]^-$;

42: Yield: 62%; White amorphous solid; M.P.: 181–183 °C; ^{1}H NMR (500 MHz, DMSO-d_6): δ3.89(s, 3H, OCH_3), 4.08(s, 2H, CH_2), 4.95(s, 2H, CH_2, benzylic), 7.00(d, 2H, 2 × CH, phenyl ring proton, *J*=8.5 Hz), 7.03 (d, 2H, 2 × CH, phenyl ring proton, *J*=8.5 Hz), 7.37–7.65(bm, 5H, 5 × CH, benzylic ring), 7.72(s, 1H, =CH, benzylidene), 7.94(s, 1H, CH, aromatic), 8.02(d, 1H, CH, *J* = 8.0 Hz, aromatic), 8.09(d, 1H, CH, aromatic, *J*=8.0 Hz), 10.97(s, 1H, –NH); ^{13}C NMR (125 MHz, DMSO-d_6): δ35.91, 55.93, 77.13, 110.26, 115.68, 125.72, 127.68, 128.35, 129.83, 130.41, 130.68, 132.64, 135.92, 136.07, 136.13, 137.27, 137.73, 153.21, 165.25, 166.98, 191.64; Electrospray mass for $C_{25}H_{21}NO_4$ (CH_3CN): Positive mode, 400$[M + H]^+$; HRMS-ESI-TOF (MeOH) for $C_{25}H_{21}NO_4$ calculated,400.1548 for $[M + H]^+$ found, 400.1505.

43: Yield: 77%; Yellowish green amorphous solid; M.P.: 249–252 °C; ^{1}H NMR (500 MHz, DMSO-d_6): δ 3.83(s, 3H, OCH_3), 3.91(s, 3H, OCH_3), 4.03(s, 2H, CH_2), 4.90(s, 2H, -OBn), 7.08(s, 1H, =CH, benzylidene proton), 7.14–7.41(bm, 5H, 5 × CH, Bn ring protons), 7.46(s, 1H, CH, aromatic proton), 7.76(d, 2H, 2 × CH, phenyl ring proton, *J*=8.0 Hz), 7.83(s, 1H, CH, aromatic proton), 8.11(d, 2H, 2 × CH, phenyl ring proton, *J*=8.0 Hz), 8.45(s, 1H, —NH); ^{13}C NMR (125 MHz, DMSO-d_6): δ48.62, 55.67, 56.07, 77.09, 104.68, 107.80, 108.12, 126.65, 127.63, 128.36, 129.87, 130.60, 132.44, 135.46, 137.35, 138.15, 144.30, 145.38, 149.39, 155.58, 162.00, 191.75. ESI-MS (MeOH) for $C_{26}H_{23}NO_5$; 429 $[M^+]$, 452$[M + Na]^+$, 468 $[M + K]^+$; Electrospray mass for $C_{26}H_{23}NO_5$ (MeOH): Positive mode, 429$[M]^+$, 452$[M + Na]^+$,

46: Yield: 66%; M.P.: 221–223 °C; ^{1}H NMR (500 MHz, DMSO-d_6): δ3.89(s, 3H, OCH_3), 4.11(s, 2H, CH_2), 4.89(s, 2H, -OCH_2Bn), 6.54(d, 1H, =CH, olefinic proton, *J* = 15.5 Hz), 7.05(d, 1H, CH, aromatic proton, *J* = 8.5 Hz), 7.19(s, 1H, CH, aromatic proton), 7.32(s, 1H, =CH, benzylidene proton), 7.37–7.46(bm, 5H, 5 × CH, Bn proton), 7.56(d, 1H, =CH, olefinic proton, *J*=15.5 Hz), 7.62(d, 1H, CH, aromatic proton, *J*=9.0 Hz), 7.70(d, 2H, 2 × CH, phenyl ring proton, *J*=8.0 Hz), 7.80(d, 2H, 2 × CH, phenyl ring proton, *J* = 8.5 Hz); ^{13}C NMR (125 MHz, DMSO-d_6): δ38.12, 55.85, 67.46, 110.21, 115.52, 122.74, 125.57, 128.21, 128.39, 130.52, 130.71, 131.09, 131.60, 135.56, 136.30,

136.53, 138.85, 153.02, 165.08, 191.36; HRMS-ESI-TOF (MeOH) for $C_{27}H_{23}NO_4$ calculated, 426.1705 for $[M + H]^+$ found, 426.1705.

47: Yield: 81%; Yellow amorphous solid; M.P.: 185–187 °C; ^{1}H NMR (500 MHz, $CDCl_3$): δ3.78(s, 2H, CH_2), 3.92(s, 3H, OCH_3), 3.99(s, 3H, OCH_3), 4.98(s, 2H, -OCH_2Bn), 6.88(d, 1H, =CH, olefinic proton, $J = 15$ Hz), 6.96(s, 1H, =CH, benzylidene proton), 7.23(s, 1H, CH, aromatic proton), 7.28(s, 1H, CH, aromatic proton), 7.30–7.64(bm, 10*H*, 9 × CH, =CH, phenyl ring + benzylidene proton), 7.80(d, 1H, Olefinic, J=15.5 Hz), 8.05(s, 1H, —NH); ^{13}C NMR (125 MHz, $CDCl_3$): δ32.20, 34.90, 56.16, 56.31, 105.15, 106.86, 107.20, 128.92, 129.31, 131.29, 131.39, 131.50, 133.60, 136.34, 136.45, 136.50, 136.63, 137.52, 141.32, 143.9, 144.79, 149.80, 155.66, 192.85; HRMS-ESI-TOF (MeOH) for $C_{28}H_{25}NO_5$ calculated, 456.1810 for $[M + H]^+$ found, 456.1800.

5.1.7. General procedure for the synthesis of compounds **12** and **44**, **45**, **48**, and **49**

Synthesis of *N*-hydroxy-3-(4-((4,5,6-trimethoxy-1-oxo-3-(3,4,5-trimethoxyphenyl)-2,3-dihydro-1H-inden-2-yl)methyl)phenyl) propanamide (**12**).

To a stirred solution of dry THF (20 mL) compound **11** was taken. To this 10% Palladium-charcoal (100 mg) was added and further stirred at RT for 2 h. On completion, reaction mixture was filtered through celite bed (Filter aid) and washed with ethyl acetate (20 mL). Organic layer was washed with water (20 mL), dried over anhydrous sodium sulphate and evaporated. The residue was charged in a silica gel column (100–200 mesh) and eluted with ethyl acetate-hexane to get the desired product at 60% ethyl acetate-hexane to get compound **12** as a viscous compound.

12: Yield: 52%; Creamy while amorphous solid; M.P.:104–107 °C; ^{1}H NMR (500 MHz, $CDCl_3$): δ2.15–3.34(bm, 6H, CH_2), 3.46(s, 3H, OCH_3), 3.72(s, 3H, OCH_3), 3.77(s, 3H, OCH_3), 3.84(s, 6H, 2 × OCH_3), 3.91(s, 3H, OCH_3), 4.12(m, 1H, 3-CH), 4.57(d, 1H, 3-CH), 5.85(s, 2H, 2 × CH, aryl proton), 6.98(d, 2H, 2 × CH, phenyl ring proton), 7.06(d, 2H, 2 × CH, phenyl ring proton), 7.25(s, 1H, CH, aromatic proton); ^{13}C NMR (125 MHz, $CDCl_3$): δ 31.52, 31.92, 45.83, 56.01, 56.11, 56.26, 60.12, 60.29, 60.98, 100.40, 104.41, 123.96, 127.92, 128.74, 129.58, 131.54, 136.38, 138.54, 139.86, 142.64, 150.06, 150.45, 152.70, 155.12, 170.00, 206.47; HRMS-ESI-TOF (MeOH) for $C_{31}H_{35}NO_9$ calculated, 564.2233 for $[M-H]^-$ found, 564.2206.

44: Yield: 62%; M.P.:146–149 °C; ^{1}H NMR (500 MHz, DMSO-d_6): δ2.73(d, 2H, CH_2, cyclopentanone ring proton, $^3J_{ab} = 5.5$ Hz, $^3J_{ac} = 4.5$ Hz), 3.03(d, 2H, CH_2, benzylic proton, $^3J_{ab}$ =5.5 Hz, $^3J_{ac}$= 4.0 Hz), 3.05–3.20(bm, 1H, 3-CH), 3.83(s, 3H, OCH_3), 6.96(d, 1H, CH, aromatic proton, $J = 8.5$ Hz), 7.04(s, 1H, CH, aromatic proton), 7.35(d, 2H, 2 × CH, phenyl ring proton, $J = 8.0$ Hz), 7.59(d, 2H, 2 × CH, phenyl ring proton, J=8.0 Hz), 7.67(d, 1H, CH, aromatic proton, J=8.0 Hz), 9.01(s, 1H, —NH); ^{13}C NMR (125 MHz, DMSO-d_6): δ 31.61, 35.95, 47.90, 55.76, 110.08, 115.59, 124.97, 126.97, 128.94, 129.17, 130.73, 143.17, 156.72, 164.18, 165.07, 204.93; ESI-MS (MeOH) for $C_{18}H_{17}NO_4$; 312 $[M + H]^+$, 334 $[M + Na]^+$, 350 $[M + K]^+$; Negative mode: 310 $[M-H]^-$.

45: Yield: 62%; light red amorphous solid; M.P.: 208–212 °C; ^{1}H NMR (500 MHz, $CDCl_3$): δ2.69–3.08(bm, 4H, 2 × CH_2), 3.34–3.38(bm, 1H, 3-CH), 3.89(s, 3H, OCH_3), 3.92(s, 3H, OCH_3), 6.79(s, 1H, CH, aromatic proton), 7.17(s, 1H, CH, aromatic proton), 7.35(d, 2H, 2 × CH, phenyl ring proton. $J = 8.0$ Hz), 7.73(d, 2H, 2 × CH, phenyl ring proton, J=8.0 Hz); ^{13}C NMR (125 MHz, $CDCl_3$): δ28.34, 32.32, 48.69, 56.11, 56.23, 104.42, 107.41, 126.06, 126.98, 128.54, 131.42, 144.25, 148.83, 149.59, 155.77, 169.44, 206.07; ESI-MS (MeOH) for $C_{19}H_{19}NO_5$; 364 $[M + Na]^+$; Negative mode: 340 $[M-H]^-$;

48:Yield: 54%; oil; ^{1}H NMR (500 MHz, $CDCl_3$): δ2.58–3.11(bm, 8H, 4 × CH_2), 3.12–3.35(bm, 1H, 3-CH), 6.82(s, 1H, CH, aromatic proton), 6.90(d, 1H, CH, aromatic proton, J=8.5 Hz), 7.13(d, 2H, 2 × CH, phenyl ring proton, J=8.0 Hz), 7.16(d, 2H, 2 × CH, phenyl ring proton, J=8.0 Hz), 7.71(d, 1H, CH, aromatic proton, J=8.5 Hz), 8.02(s, 1H, —NH); ^{13}C NMR (125 MHz, $CDCl_3$): δ30.23, 31.92, 35.44, 36.83, 49.06, 55.61, 109.73, 115.39, 125.76, 128.39, 129.10, 129.80, 137.79, 138.21, 156.66, 165.47, 177.75, 206.14; HRMS-ESI-TOF (MeOH) for $C_{20}H_{21}NO_4$ calculated, 338.1392 for $[M-H]^-$ found, 338.1405; ESI-MS (MeOH) for $C_{20}H_{21}NO_4$; 339 $[M^+]$.

49: Yield: 52%; oil; ^{1}H NMR (500 MHz, DMSO-d_6): δ2.54–2.99(bm, 8H, 4 × CH_2), 3.01–3.11(bm, 1H, 3-CH), 3.83(s, 6H, 2 × OCH_3), 7.06(s, 1H, CH, aromatic proton), 7.08(s, 1H, CH, aromatic proton), 7.11(d, 2H, 2 × CH, phenyl ring proton, J=8.0 Hz), 7.16(d, 2H, 2 × CH, phenyl ring proton, J=8.0 Hz), 8.73(s, 1H, —NH); ^{13}C NMR (125 MHz, DMSO-d_6): δ30.43, 31.26, 33.83, 35.91, 48.26, 55.63, 55.92, 103.96, 108.26, 128.46, 128.86, 132.26, 137.25, 138.80, 148.84, 149.15, 155.32, 168.34, 205.49; HRMS-ESI-TOF (MeOH) for $C_{21}H_{23}NO_5$ calculated, 392.1473 for $[M + Na]^+$ found, 392.1476.

5.1.8. Synthesis of (E)-N-Hydroxy-3-(4-((Z)-(4,5,6-trimethoxy-1-oxo-3-(3,4,5-trimethoxyphenyl)-1H-inden-2(3H)-ylidene) methyl) phenyl-prop-2-enamide(**10**)

To a stirred solution of dry chloroform (10 mL), compound **9** (100 mg, 0.18 mmol), DMAP (30 mg, 0.24 mmol) and acetic anhydride (0.1 mL, 108 mg, 1.06 mmol) were added and further stirred at RT for 2 h. On completion, reaction mixture was acidified with 5% HCl (10 mL) and extracted with chloroform (15 mLx2). Combined organic layer was washed with water (20 mLx2), dried over anhydrous sodium sulphate and dried in vacuo. The residue was recrystallized from chloroform-hexane to get acetylated derivative **10** as amorphous solid.

Yield: 99 mg (92%); M.P.: 93–96 °C; ^{1}H NMR (500 MHz, $CDCl_3$): δ2.23(s, 3H, CH_3), 3.46(s, 3H, OCH_3), 3.74(s, 6H, 2 × OCH_3), 3.76(s, 3H, OCH_3), 3.92(s, 3H, OCH_3), 3.94(s, 3H, OCH_3), 5.31(s, 1H, 3-CH), 6.38–6.46(bd, 3H, =CH, 2 × CH, olefinic + aryl proton), 7.24(s, 1H, CH, aromatic proton), 7.45(d, 2H, 2 × CH, J=8.0 Hz), 7.54(d, 2H, 2 × CH, J=8.5 Hz), 7.67(s, 1H, =CH, benzylidene proton), 7.70(s, 1H, olefinic CH); ^{13}C NMR (125 MHz, $CDCl_3$): δ23.44, 30.30, 31.94, 32.21, 33.84, 46.25, 51.85, 56.21, 56.32, 60.31, 60.91, 60.96, 101.45, 105.92, 114.08, 118.92, 125.03, 127.96, 131.55, 133.40, 135.24, 136.78, 140.88, 140.97, 143.71, 149.97, 153.05, 155.02, 167.19, 193.61; Electrospray mass for $C_{33}H_{33}NO_{10}$ (CH_3CN): Positive mode, 604$[M + H]^+$, 626$[M + Na]^+$, 642$[M + K]^+$.

23: Yield: 58%; oil; ^{1}H NMR (500 MHz, $CDCl_3$):δ 2.79(dd, 1H, CH_2, benzylic proton), 2.88 (dd, 1H, CH_2, benzylic proton), 3.33(s, 3H, OCH_3), 3.39(s, 3H, OCH_3), 3.57(s, 3H, OCH_3), 3.74(s, 3H, OCH_3), 3.79 (s, 3H, OCH_3), 3.88(s, 3H, OCH_3), 3.93(s, 3H, OCH_3), 4.09–4.10(bm, 1H, 3-CH), 4.56(d, 1H, 3-CH), 5.82(s, 2H, 2 × CH, aryl proton), 7.29(d, 2 × CH, phenyl ring proton, J=8.0 Hz), 7.86(s, 1H, CH, aromatic proton), 7.93(d, 2 × CH, phenyl ring proton, J=8.5 Hz); ^{13}C NMR (125 MHz, $CDCl_3$): δ52.07, 56.24, 56.26, 56.30, 59.30, 60.36, 60.97, 100.39, 104.04, 127.94, 128.62, 129.47, 131.40, 135.73, 136.56, 137.00, 139.57, 142.71, 144.70, 145.68, 148.81, 150.47, 153.10, 155.19, 167.00, 205.85; ESI-MS (MeOH): for $C_{30}H_{32}O_9$; 537 $[M + H]^+$, 559 $[M + K]^+$, 573 $[M + K]^+$.

5.2. Biological evaluation

Detailed biological procedures are given in Supplementary information.

5.2.1. Antiproliferative activity by Sulphorhodamine assay

In vitro cytotoxicity SRB assay was performed as described previously.[46] Doxorubicin, podophyllotoxin, tamoxifen and tubastatin A were used as positive controls.

5.2.2. Cell cycle analysis

Cell cycle analysis was performed with MDA-MB-231 and K-562 cell following the reported protocol.[47] Doxorubicin was used as positive controls.

5.2.3. Tubulin polymerisation assay

Tubulin Polymerization assay was performed using 'assay kit-BK-

006P' from Cytoskeleton, USA, as per Manufacturer's protocol.[48] Paclitaxel was used as a standard stabilizer of tubulin polymerase and podophyllotoxin (PDT) as standard inhibitor.

5.2.4. HDAC inhibition assay

The HDACs inhibitor activity of the compounds was evaluated by using both the HeLa nuclear extract as source of class I/II HDAC enzymes and the human recombinant HDAC6 enzyme.[49]

The HDAC activity of HeLa nuclear extract was assessed by using the fluorometric HDAC Inhibitor Drug Screening Kit (BioVision, catalog #K340-100) according to the procedures recommended by the manufacturer. Trichostatin A and Tubastatin A were used as positive controls.

5.2.5. Confocal microscopy imaging

Experiment was performed with HeLa cells, cells were stained withAlexa Fluor® 488 mouse anti-β-tubulin (BD Pharmingen™). Images were acquired through a 60 CFI Plan Apochromat Nikon objectives with a Nikon C1 confocal microscope.

5.2.6. Molecular docking studies

(a) *Interaction with β-tubulin and HDAC1 & HDAC6:* The 3D crystallographic structure of protein target β-tubulin, HDAC1 & HDAC6 complexed with ligands were retrieved from protein Data Bank (PDB) (https://www.pdb.org). Molecular docking study were done by using Autodock Vina v0.8 (Molecular Graphics Lab at The Scripps Research Institute, La Jolla, CA 92037, USA).[50]

(b) *Prediction of physicochemical properties:* The physicochemical properties of compound **21** were assessed by using SwissADME online software.[51] Highly selective HDAC6 clinical drug Tubastatin A was used for comparison. Physicochemical properties, 'Lipinski rule of 5′, Water solubility, Lipophilicity, Pharmacokinetics, Drug likeness, Pan-Assay Interference Compounds (PAINS) and then bioavailability score.

5.2.7. In-vitro antiinflammatory activity

Antiinflammatory assay was assessed on Lipopolysaccharide (LPS) induced primary macrophages cells as per our reported method.[52] TNF-α and IL-6 released in the cell culture supernatant were determined with ELISA kits procured from BD Biosciences, USA.

5.2.8. Safety studies by acute oral toxicity

Safety evaluation was done as per reported method.[53] Compound **21** was given through oral route at four different single acute dose at 5 mg/kg, 50 mg/kg, 300 mg/kg, and 1000 mg/kg to Swiss albino mice (n = 6). The toxicity study and number of animals used were approved *via* CIMAP/IAEC/2016–19/32 dated 09–02-2017 by the Institutional Animal Ethics Committee (IAEC) of CSIR-Central Institute of Medicinal and Aromatic Plants, Lucknow, India.

5.2.9. Statistical analysis

All data have been expressed as mean ± standard deviation (SD) were calculated using MS-Excel. Statistical analysis of differences was carried out by ANOVA. For acute oral toxicity data expressed in ± SE, Comparisons are made relative to the untreated controls. Differences with a p value < 0.05 were considered significant.

Declaration of Competing Interest

The authors declare that they have no known competing financial interests or personal relationships that could have appeared to influence the work reported in this paper.

Data availability

Selective important data has been shared. Supplementary file is being submitted

Acknowledgement

The study was financially supported from Indo-Italian Bilateral project under GAP-392. Kapil Kumar acknowledges to UGC for their Senior Research Fellowships and Barsha Thapa acknowledges to DBT for Junior Research Fellowship. Biological Central Facility and Chemical Central Facility of CSIR-CIMAP are duly acknowledged for Sophisticated Instrumentation support. CIMAP Communication No.: CIMAP/PUB/2023/08

Appendix A. Supplementary material

Supplementary data to this article can be found online at https://doi.org/10.1016/j.bmc.2023.117300.

References

1 Liu W, Wang X, Zhu H, Duan Y. Precision tumor medicine and drug targets. *Curr Top Med Chem*. 2019;19:1488–1489.
2 Kamb A, Wee S, Lengauer C. Why is cancer drug discovery so difficult? *Nat Rev Drug Discov*. 2007;6:115–120.
3 Anighoro A, Bajorath J, Rastelli G. Polypharmacology: challenges and opportunities indrug discovery. *J Med Chem*. 2014;57:7874–7887.
4 Lu DY, Lu TR, Yarla NS, et al. Drug combination in clinical cancer treatments. *Rev Rec Clin Trials*. 2017;12:202–211.
5 Shaveta MS, Singh P. Hybrid molecules: the privileged scaffolds for various pharmaceuticals. *Eur J Med Chem*. 2016;124:500–536.
6 Bedard PL, Hyman DM, Davids MS, Siu LL. Small molecules, big impact: 20 years of targeted therapy in oncology. *Lancet*. 2020;395:1078–1088.
7 Proschak E, Stark H, Merk D. Polypharmacology by Design: A Medicinal Chemist's Perspective on Multitargeting Compounds. *J Med Chem*. 2019;62:420–444.
8 Roche J, Bertrand P. Inside HDACs with more selective HDAC inhibitors. *Eur J Med Chem*. 2016;121:451–483.
9 Moniot S, Weyand M, Steegborn C. Structures, substrates, and regulators of Mammalian sirtuins opportunities and challenges for drug development. *Front Pharmacol*. 2012;3:16.
10 New M, Olzscha H, La Thangue NB. HDAC inhibitor-based therapies: Can we interpret the code? *Mol Oncol*. 2012:637–1356.
11 Choudhary C, Kumar C, Gnad F, et al. Lysine acetylation targets protein complexes and co-regulates major cellular functions. *Science*. 2009;325:834–840.
12 Marks P, Rifkind RA, Richon VM, Breslow R, Miller T, Kelly WK. Histone deacetylases and cancer: causes and therapies. *Nat Rev Cancer*. 2001;1:194–202.
13 Schemies J, Sippl W, Jung M. Histone deacetylase inhibitors that target tubulin. *Cancer Lett*. 2009;280:222–232.
14 Marks PA. The clinical development of histone deacetylase inhibitors as targeted anticancer drugs. *Expert Opin Invest Drugs*. 2010;19:1049–1066.
15 Peng X, Sun Z, Kuang P, Chen J. Recent progress on HDAC inhibitors with dual targeting capabilities for cancer treatment. *Eur J Med Chem*. 2020;208, 112831.
16 Wang Y, Sun M, Wang Y, et al. Discovery of novel tubulin/HDAC dual-targeting inhibitors with strong antitumor and antiangiogenic potency. *Eur J Med Chem*. 2021;225, 113790.
17 Shuai S, Yan X, Zhang J, et al. TIP30 nuclear translocation negatively regulates EGF-dependent cyclin D1 transcription in human lung adenocarcinoma. *Canc Lett*. 2014;354:200–209.
18 Sudo T, Mimori K, Nishida N, et al. Histone deacetylase 1 expression in gastric cancer. *Oncol Rep*. 2011;26:777–782.
19 Zhang Z, Yamashita H, Toyama T, et al. Quantitation of HDAC1 mRNA expression in invasive carcinoma of the breast. *Breast Canc Res Treat*. 2005;94:11–16.
20 Halkidou K, Gaughan L, Cook S, Leung HY, Neal DE, Robson CN. Upregulation and nuclear recruitment of HDAC1 in hormone refractory prostate cancer. *Prostate*. 2004;59:177–189.
21 Liu X, Wang JH, Li S, et al. Histone deacetylase 3 expression correlates with vasculogenic mimicry through the phosphoinositide3-kinase/ERK-MMP-laminin5g2 signaling pathway. *Canc Sci*. 2015;106:857–866.
22 Zhang Z, Yamashita H, Toyama T, et al. HDAC6 expression is correlated with better survival in breast cancer. *Clin Canc Res*. 2004;10:6962–6968.
23 Brindisi M, Saraswati AP, Brogi S, Gemma S, Butini S, Campiani G. Old but Gold: Tracking the New Guise of Histone Deacetylase 6 (HDAC6) Enzyme as a Biomarker and Therapeutic Target in Rare Diseases. *J Med Chem*. 2020;63:23–39.
24 Grant S, Easley C, Kirkpatrick P. Vorinostat. *Nat Rev Drug Discov*. 2007;6:21–22.
25 Hood K, Shah A. Belinostat for Relapsed or Refractory Peripheral T-Cell Lymphoma. *J Adv Pract Oncol*. 2016;7:209–218.
26 Bailey H, Stenehjem DD, Sharma S. Panobinostat for the treatment of multiple myeloma: the evidence to date. *Hematol Res Rev*. 2015;6:269–276.
27 Chan TS, Tse E, Kwong YL. Chidamide in the treatment of peripheral T-cell lymphoma. *Onco Targets Ther*. 2017;10:347–352.
28 Shah RR. Safety and tolerability of histone deacetylase (HDAC) inhibitors in oncology. *Drug Saf*. 2019;42:235–245.

29 Singh A, Fatima K, Singh A, et al. Anticancer activity and toxicity profiles of 2-benzylidene indanone lead Molecule. *Eur J Pharm Sci.* 2015;76:57–67.
30 Verma AK, Fatima K, Dudi RK, et al. Antiproliferative activity of diarylnaphthylpyrrolidine derivative *via* dual target inhibition. *Eur J Med Chem.* 2020;188, 111986.
31 Negi AS, Gautam Y, Alam S, et al. Natural antitubulins: importance of 3,4,5-trimethoxyphenyl fragment. *Bioorg Med Chem.* 2015;23:373–389.
32 Hinshaw DC, Shevde LA. The Tumor Microenvironment Innately Modulates Cancer Progression. *Cancer Res.* 2019;79:4557–4566.
33 Furman D, Campisi J, Verdin E, et al. Chronic inflammation in the etiology of disease across the life span. *Nat Med.* 2019;25:1822–1832.
34 Janke C, Magiera MM. The tubulin code and its role in controlling microtubule properties and functions. *Nat Rev Mol Cell Biol.* 2020;21:307–326.
35 Liu Y, Li L, Min J. HDAC6 finally crystal clear. *Nat Chem Biol.* 2016;12:660–661.
36 Shen S, Svoboda M, Zhang G, et al. Structural and *in vivo* characterization of tubastatin A, a widely used histone deacetylase 6 Inhibitor. *ACS Med Chem Lett.* 2020;11:706–712.
37 Segeren HA, Westendorp B. Mechanisms used by cancer cells to tolerate drug-induced replication stress. *Cancer Lett.* 2022;544:15804.
38 Cao YN, Zheng LL, Wang D, Liang XX, Zhou GF, Xl.. Recent advances in microtubule-stabilizing agents. *Eur J Med Chem.* 2018;143:806–828.
39 Brouhard GJ, Rice LM. Microtubule dynamics: an interplay of biochemistry and mechanics. *Nat Rev Mol Cell Biol.* 2018;19:451–463.
40 Field JJ, Díaz JF, Miller JH. The binding sites of microtubule-stabilizing agents. *Chem Biol.* 2013;20:301–315.
41 Prota AE, Bargsten K, Zurwerra D, et al. Molecular mechanism of action of microtubule-stabilizing anticancer agents. *Science.* 2013;339:587–590.
42 Ray A. Beyond debacle and debate: developing solutions in drug safety. *Nat Rev Drug Discov.* 2009;8:775–779.
43 OECD Guidelinws: Test no. 423: Acute Oral Toxicity, 08 Feb 2002:1-14.
44 WHO: Pharmacovigilance indicators: a practical manual for the assessment of pharmacovigilance systems. 2015. Geneva, Switzerland. Pp. 1-73, ISBN 978924150825.
45 Srivastava A, Ravi K, Fatima K, et al. 3-Arylindanones and related compounds as antiproliferative agents against colorectal cancer. *Chem Biol Drug Design.* 2019;94:1694–1705.
46 Vichai V, Kritikara K. Sulforhodamine B Colorimetric Assay for Cytotoxicity Screening. *Nat Protoc.* 2006;1:1112–1116.
47 Hussain MK, Singh DK, Singh A, et al. *Sci Rep.* 2017;7:10864–110863.
48 Khwaja S, Fatima K, Hassanain BC, et al. Antiproliferative efficacy of curcumin mimics through microtubule destabilization. *Eur J Med Chem.* 2018;151:51–61.
49 Santo L, Hideshima T, Kung AL, et al. Preclinical activity, pharmacodynamic and pharmacokinetic prioperties of a selective HDAC 6 inhibitor, ACY-1215, in combination with bortezomib in multiple myeloma. *Blood.* 2012;119:2579–2589.
50 Trott O, Olson AJ. AutoDockVina: improving the speed and accuracy of docking with a new scoring function, efficient optimization, and multithreading. *J Comp Chem.* 2010;31:455–461.
51 http://www.swissadme.ch/, access 2021.
52 Pathak N, Fatima K, Singh S, et al. Bivalent furostene carbamates as antiproliferative and antiinflammatory Agents. *J St Biochem Mol Biol.* 2019;194, 105457.
53 Chanda D, Shanker K, Pal A, et al. Safety evaluation of Trikatu: a generic Ayurvedic medicine in Charles Foster rats. *J Toxicol Sci.* 2009;34:99–108.